



HAL
open science

Vegetation and fire variability in the central Cerrados (Brazil) during the Pleistocene-Holocene transition was influenced by oscillations in the SASM boundary belt

Raquel Franco Cassino, Marie-Pierre Ledru, Rudney de Almeida Santos,
Charly Favier

► To cite this version:

Raquel Franco Cassino, Marie-Pierre Ledru, Rudney de Almeida Santos, Charly Favier. Vegetation and fire variability in the central Cerrados (Brazil) during the Pleistocene-Holocene transition was influenced by oscillations in the SASM boundary belt. *Quaternary Science Reviews*, 2020, 232, pp.106209. 10.1016/j.quascirev.2020.106209 . hal-02484480

HAL Id: hal-02484480

<https://hal.science/hal-02484480>

Submitted on 10 Dec 2020

HAL is a multi-disciplinary open access archive for the deposit and dissemination of scientific research documents, whether they are published or not. The documents may come from teaching and research institutions in France or abroad, or from public or private research centers.

L'archive ouverte pluridisciplinaire **HAL**, est destinée au dépôt et à la diffusion de documents scientifiques de niveau recherche, publiés ou non, émanant des établissements d'enseignement et de recherche français ou étrangers, des laboratoires publics ou privés.

1 **Vegetation and fire variability in the central Cerrados (Brazil) during the Pleistocene-Holocene**
2 **transition was influenced by oscillations in the SASM boundary belt**

3 **Quaternary Science Reviews Volume 232, 15 March 2020, 106209**

4 <https://doi.org/10.1016/j.quascirev.2020.106209>

5 Raquel Franco Cassino ^{(1)*}; Marie-Pierre Ledru ⁽²⁾; Rudney de Almeida Santos ^(2,3); Charly Favier ⁽²⁾

6 ⁽¹⁾Departamento de Geologia, Universidade Federal de Ouro Preto, Brazil; ⁽²⁾Institut des Sciences de
7 l'Évolution de Montpellier, Université de Montpellier CNRS IRD EPHE, France; ⁽³⁾Universidade de São
8 Paulo, Brazil.

9 *corresponding author (address: Departamento de Geologia, Universidade Federal de Ouro
10 Preto/Campus Morro do Cruzeiro, Bauxita, 35400-000, Ouro Preto, Brazil. E-mail address:
11 raquelcassino@ufop.edu.br)

12 **Abstract**

13 This study investigates historical fire regimes and arboreal cover variability in the Brazilian Cerrados, a
14 large Neotropical savanna ecosystem, during the Pleistocene-Holocene transition and early Holocene, and
15 then tests whether the observed variation is linked to South American Summer Monsoon (SASM)
16 variability. We present high-resolution pollen, XRF and charcoal records from lake Lagoa Feia, located in
17 central Cerrados, and assess how they compare with other pollen records from the surrounding region to
18 investigate regional trends of vegetation and fire regime variability. Our results show that the Pleistocene-
19 Holocene transition was marked by a wet episode, which included moist forest expansion and rising lake
20 levels, that correlates well with increased monsoon activity in a large area of central South America during
21 the same period. This wet episode chronologically coincides with the Younger Dryas cold episode in the
22 northern hemisphere. Our data revealed moisture declines in central Cerrados after 11.2 kyr BP, along
23 with centennial-scale fluctuations from dry to wet conditions throughout the early Holocene period until
24 around 6 kyr BP. These dry/wet oscillations are associated with weakened SASM activity and repeated
25 shifts of its belt position during this time range. Fire activity increased in central Cerrados just after the
26 onset of drier conditions during the early Holocene, and likely contributed to decreased arboreal cover at
27 that time. A trend of increasing moisture in the region was observed after 6 kyr BP. Our study reveals how
28 centennial and millennial-scale changes in monsoon activity influenced arboreal cover, diversity and fire
29 regimes in the central Cerrados.

30 **Keywords: Brazil; Termination 1; fire; pollen; tropical savanna; Paleoclimatology**

31 **1. Introduction**

32 The Brazilian Cerrados is the second largest biome of the Neotropics, covering about 2 million
33 km² of tropical South America (Fig. 1A). The vegetation of the Cerrados is classified as a moist savanna and
34 comprises open savannas, savanna woodlands, grasslands and shrubby grasslands, dry forests and
35 riverine forests (Furley, 1999). The wide range of latitudes - 2° to 24°S – across which this biome stretches
36 entails significant climatic variability across the region, but the occurrence of a strong dry season during

37 austral winter (usually spanning four to six months) is common to the whole biome (Oliveira-Filho &
38 Ratter, 2002; Fig. 1B). Rainfall is concentrated in the austral summer months, and is influenced by South
39 American Summer Monsoon (SASM) activity (Silva & Kousky, 2012). The distribution of the Cerrados also
40 coincides with the highly weathered, nutrient-poor soils found in the plateaus of central Brazil (Motta *et*
41 *al.*, 2002, Oliveira-Filho & Ratter, 2002). In addition to rainfall seasonality and dystrophic soils, fire is an
42 important factor in the maintenance of the physiognomic and floristic diversity of the Cerrados (Hoffman
43 & Moreira, 2002). Most of the flora found in the Cerrados is adapted to, or dependent on, fire; as such,
44 the origin and diversification of these plant lineages are, to a great extent, related to fire-resistant
45 adaptations (Simon *et al.*, 2009).

46 Past changes in the structure and composition of vegetation cover in the Cerrados can be
47 considered a result of variations in rainfall amount and seasonality and/or of changes in the fire regime.
48 SASM activity is known to have varied at the millennial scale as a response to variations in Southern
49 Hemisphere (SH) insolation, which occur at orbital cycles of *ca.* 20 kyr (Kutzbach *et al.*, 2008). SASM
50 activity and SH insolation are positively correlated in that monsoon circulation and precipitation in the SH
51 is enhanced when SH insolation is at a maximum (Cruz *et al.*, 2005; Kutzbach *et al.*, 2008). Increased SASM
52 convective activity is caused by modifications in the interhemispheric temperature gradient – which is
53 significantly controlled by summer insolation – that results in southward shifts of the Intertropical
54 Convergence Zone (ITCZ) and South Atlantic Convergence Zone (SACZ) (Cheng *et al.*, 2013; Schneider *et*
55 *al.*, 2014), main features of the SASM system. Other mechanisms besides insolation variability have also
56 been documented to affect the interhemispheric temperature gradient, as well as influence the ITCZ/SACZ
57 systems; for example, Heinrich events of massive ice melting in the North Atlantic have also been related
58 to SASM variability (Kutzbach *et al.*, 2008; Strikis *et al.*, 2015; Rojas *et al.*, 2016).

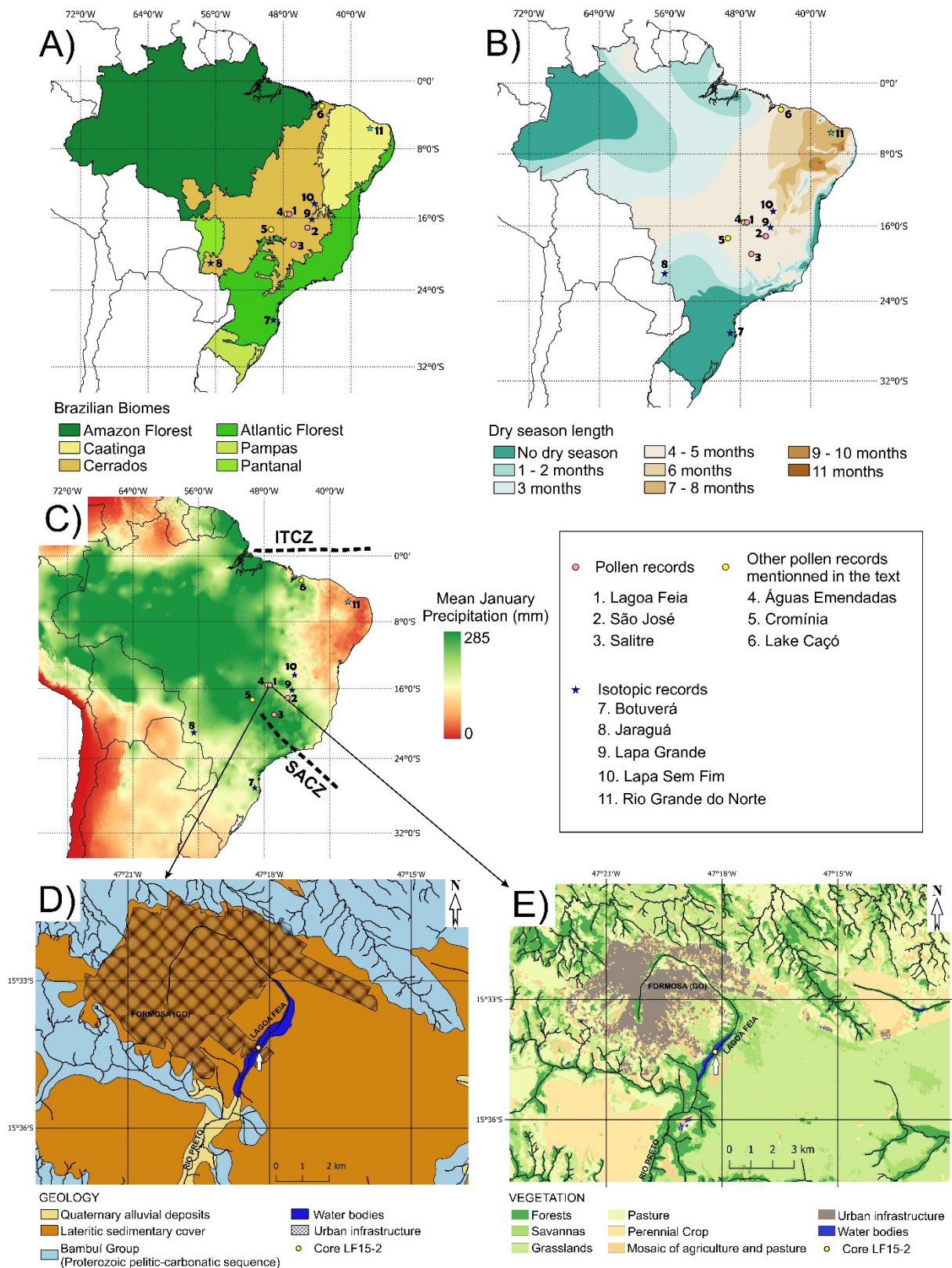
59 Late Quaternary speleothem δO^{18} records from southern Brazil (Botuverá cave (Cruz *et al.*, 2005;
60 Wang *et al.*, 2007)), central-western Brazil (Jaraguá cave (Novello *et al.*, 2017), and central-eastern Brazil
61 (Lapa Grande and Lapa Sem Fim caves (Strikis *et al.*, 2015; 2018) have been used to track changes in SASM
62 position and activity over the last glacial cycle because they show significant co-variance with SH summer
63 insolation and/or cold episodes in the North Atlantic. These speleothem records show differences that are

64 related to their latitude (from northern to southern Brazil) and, as such, can be used to infer shifts in
65 SASM belt activity and amplitude (Maslin *et al.*, 2011).

66 Speleothem records show a succession of wet/dry events during the late Pleistocene and
67 Holocene. Dry events with reduced rainfall over central and southern SASM regions were observed during
68 warmer NH conditions (14.7 to 12.9 kyr BP) (Wang *et al.*, 2007; Novello *et al.*, 2017), while the return of
69 colder NH conditions during the Younger Dryas event (12.9 to 11.7 kyr BP) resulted in increased moisture
70 across southern, central-eastern and western South America (Wang *et al.*, 2007; Novello *et al.*, 2017;
71 Stríkis *et al.*, 2018). During the early Holocene, the onset of relatively drier conditions in the SASM region
72 was again correlated with warmer NH conditions (Novello *et al.*, 2017; Cruz *et al.*, 2005). From the middle
73 Holocene onwards, a general trend towards wetter conditions was observed in southern Brazil (Cruz *et al.*,
74 2005). Conversely, in the eastern Amazon, the speleothem record from the Paraíso cave (Wang *et al.*,
75 2017) shows peak of high humidity around 6,000 yr BP and then a tendency of decrease in rainfall amount
76 until the present. In central-eastern Brazil, the Holocene was punctuated by abrupt fluctuations in wet
77 and dry events, with the early and middle Holocene showing longer wet events than the late Holocene
78 (from 4.0 kyr BP onwards) (Stríkis *et al.*, 2011).

79 The present study aims to discuss how SASM variability has affected the fire activity and
80 vegetation of the central Cerrados during the Pleistocene/Holocene transition and the early Holocene.
81 Our discussion is based on a new high-resolution pollen, charcoal and XRF record from Lagoa Feia, which
82 is located near Brasília in the core region of the Brazilian Cerrados. Lagoa Feia represents the first record
83 from the central area of the Cerrados that covers the early Holocene, as previously published records
84 from this region include hiatuses or no pollen record at the end of the Pleistocene and early Holocene
85 (Salgado-Labouriau *et al.*, 1997a; Barberi *et al.*, 2000). The Lagoa Feia record provides unprecedented
86 insight into landscape and rainfall variability in central Brazil. We have assessed the regional scope of
87 these variations, along with their implications for SASM boundary belt oscillations based on comparisons
88 with other pollen and paleoclimatic records from the Cerrados and adjacent regions.

89



90

91 **Figure 1:** Geographic distribution and climate of the Cerrados, locations from which pollen (Lagoa Feia (this
 92 study); São José (Cassino *et al.*, 2018); Salitre (Ledru, 1993; Ledru *et al.*, 1996); Águas Emendadas (Barberi *et al.*,
 93 2000); Cromínia (Salgado-Labouriau *et al.*, 1997); Lake Caçó (Ledru *et al.*, 2006)) and isotopic records (Botuverá
 94 (Cruz *et al.*, 2005; Wang *et al.*, 2007); Jaraguá (Novello *et al.*, 2017); Lapa Grande/Lapa Sem Fim (Stríkis *et al.*,
 95 2015); Rio Grande do Norte (Cruz *et al.*, 2009)) mentioned in this study were collected, and geology and
 96 vegetation of the Lagoa Feia site. A) Distribution of Brazilian biomes (from IBGE, 2004); B) Map of the length of
 97 the dry season across Brazil (from IBGE, 2002); C) Mean January precipitation in South America during the apex

7

8

4

98 of the SASM season (from Fick & Hijmanns, 2017); D) Geological map of the region around Lagoa Feia (from
99 Lacerda Filho *et al.*, 2000); E) Vegetation map of the region around Lagoa Feia (from Project MapBiomass, 2019).

100
101

2. Vegetation and Climate in the Cerrados

102 The Brazilian Cerrados extends from the equatorial zone to around 24° south latitude in Central
103 Brazil. As such, the Cerrados includes transitional areas with four other Brazilian biomes, namely, the
104 Amazon Forest to the north, the Caatinga to the northeast, the Atlantic Forest to the east and the
105 Pantanal to the west (Fig. 1A).

106 The Cerrados demonstrates high physiognomic diversity as the region includes forests, savannas
107 and grasslands. The Cerrados contains two different kinds of forest formations: gallery, or riverine, forests
108 that follow streams and rivers and the dry forests. The dense canopy of the gallery forests maintains
109 constant moisture, even during the dry season; for this reason, the trees are usually tall and not
110 deciduous, with Apocynaceae, Fabaceae, Lauraceae and Rubiaceae the most represented families (Ribeiro
111 & Walter, 2008). The dry forests are mainly deciduous, occurring either on well-drained and nutrient-rich
112 soils or more dystrophic soils. The most common tree species (e.g. *Caryocar brasiliense*, *Qualea*
113 *grandiflora*) in dry forests are also found on savanna formations (Ribeiro & Walter, 2008).

114 The savanna formations (called *Cerrado stricto sensu*) have clearly delimited arboreal and
115 shrubby-herbaceous strata (Ribeiro & Walter, 2008), with arboreal cover ranging from 5% (sparse
116 Cerrado) to 50% (dense Cerrado). High floristic diversity is encountered on the *Cerrado stricto sensu*; for
117 example, when Ratter *et al.* (1996) compared around 100 floristic surveys from this formation, they found
118 that from a total of around 530 species only 26 (e.g. *Astronium fraxinifolium*, *Bowdichia virgiloides*,
119 *Byrsonima coccolobifolia*, *Caryocar brasiliense*, *Roupala montana*, *Tabebuia aurea*) were identified in at
120 least 50% of the surveys.

121 In addition, grassland formations, with Poaceae, Asteraceae and Cyperaceae the most
122 represented families, are differentiated according to the presence or absence of a shrubby stratum.

123 The most remarkable feature of the climate of the Cerrados is rainfall seasonality (Fig. 1B).
124 According to the Koppen criteria, most of the Cerrados region is classified as Aw, i.e. Tropical climate
125 which includes a dry austral winter (Alvares *et al.*, 2013) extending four to six months that is characterized
126 by severe water deficiency. The rainy season starts in September-October and ends in March-April, with

127 its apex between November-January when around 50% of annual rainfall occurs (Fig. 1C) (Silva *et al.*,
128 2008). The apex of the austral summer rainy season corresponds to the mature phase of the SASM, which
129 occurs between November and February. During this time, deep convection occurs over Central Brazil
130 (Vera *et al.*, 2006). Total annual precipitation in most of the Cerrados ranges between 1,000 to 1,800 mm,
131 but some areas in eastern Cerrados, especially those at the transition zone with Caatinga, receive only
132 400 to 600 mm of precipitation per year. On the other hand, more than 2,000 mm of annual precipitation
133 has been registered in some areas of northwestern Cerrados (Silva *et al.*, 2008). Mean annual
134 temperature in the Cerrados varies from 18-19°C in the southeast to 26-27°C in the northeastern area of
135 the biome (Silva *et al.*, 2008). Thermal amplitude between months in the Cerrados is relatively low, as the
136 mean minimum temperature never falls below 14°C while the mean maximum temperature never
137 exceeds 33°C (Silva *et al.*, 2008).

138 **3. Materials and Methods**

139 *3.1. Lagoa Feia record*

140 *3.1.1. Settings*

141 Lagoa Feia is an elongated lake about 3 km long in the NE-SW direction and about 140 m wide. It
142 is located in the city of Formosa (Goiás State), which is close to the Brazilian capital, Brasília. It is
143 connected to a small drainage upstream and is the source of the Rio Preto (Fig. 1D). The water is about 5
144 m deep at the center of the lake, with aquatic plants currently covering a large part of the lake's surface.

145 Lagoa Feia is located on a plateau at an altitude of around 900 m that is composed of lateritic
146 sedimentary soil that overlies a Proterozoic pelitic-carbonatic sequence of the Bambuí Group (Fig. 1D).
147 The lake may have been formed through sub-superficial carbonate dissolution, which caused local
148 subsidence of the plateau (Ferraz-Vicentini, 1999). The urban area of Formosa extends on the west side of
149 the lake, while there is a very large (1,100 Km²) uninhabited, preserved area belonging to the Brazilian
150 Army on the east side of the lake. In this area, vegetation is composed of patches of grasslands and open
151 savannas, with marshes present on depressed areas of the plateau (Fig. 1E). Forests occur along the
152 drainage area and on the sloping hillsides downstream of Lagoa Feia.

153 Regarding climatic conditions, the Lagoa Feia region has a mean annual precipitation of around
154 1,500 mm, a mean maximum temperature of 26°C and a mean minimum temperature of 14°C (according
155 to meteorological data for the last ten years, available on BDMEP/INMET - Instituto Nacional de
156 Meteorologia (<http://www.inmet.gov.br>)).

157
158 3.1.2. *Chronology, pollen, charcoal and XRF scanning*

159 A 500-cm deep core, Core LF15-2, was collected from the center of Lagoa Feia, at 15°34'S,
160 47°18'W, with a Livingstone corer in 2015. A total of 24 samples from the upper 435 cm underwent
161 radiocarbon dating by Accelerator Mass Spectrometry (Table 1) at the French *Laboratoire de Mesure du*
162 *Carbone 14* (LMC14) – UMS 2572 (CEA/DSM, CNRS, IRD, IRSN, dates from bulk samples). The age-depth
163 model was built with Bacon (Blaauw & Christen, 2011), using the calibration curve SHcal13 (Hogg *et al.*,
164 2013) (Fig. 2), and with “boundaries” set at 415.5 and 437 cm; other parameters were kept as default.

165 Subsamples of 0.5 cm³ taken about every 4 cm were prepared for pollen analysis using standard
166 methods (eg. Bennet & Willis, 2001), including treatment with HF-40%, HCl-30%, KOH-10% and acetolysis.
167 After each treatment, samples were centrifuged to concentrate the pollen grains; no sieving was used in
168 the process so that palynomorphs of all sizes were retained. Spores of the marker *Lycopodium clavatum*
169 (Stockmarr, 1971) were added prior to treatment for concentration calculations. Following analyses, 32
170 subsamples from a total of 111 subsamples presented very low pollen concentrations and were
171 considered sterile. In the other samples, at least 300 terrestrial pollen grains - excluding aquatic and
172 water-level-related taxa (e.g. Cyperaceae) - were counted. Pollen, spore and other palynomorph
173 percentages were calculated relative to the terrestrial pollen sum. Pollen diagrams were plotted with C2
174 software (Juggins, 2007), and zonation was based on constrained hierarchical clustering that applied the
175 Coniss method and included all terrestrial pollen taxa on the analysis. Pollen data from the Lagoa Feia
176 record was compared with data from the Salitre (Ledru, 1993; Ledru *et al.*, 1996) and São José (Cassino *et*
177 *al.*, 2018) pollen records to evaluate the regional significance of vegetation changes. New age-depth
178 models were generated for these two cores with Bacon (Blaauw & Christen, 2011), using the calibration
179 curve SHcal13 (Hogg *et al.*, 2013; Supplementary Material Fig. 5-6). Pollen percentages were recalculated
180 from pollen counts for the Salitre and São José records using as reference the terrestrial pollen sum.

181 Pollen data from the three sites were then summarized using four curves: % Grassland taxa
182 (*Alternanthera*; Asteraceae; *Cuphea*; *Drosera*; Eriocaulaceae; *Galianthe*; Poaceae; *Xyris*); % Savanna taxa
183 (*Astronium*-Type; *Borreria*-Type; *Byrsonima*; *Caryocar*; *Cupania*; *Forsteronia*-Type; *Matayba*; *Mimosa*-
184 Type; Myrtaceae; *Plenckia*; *Richardia*; *Roupala*; *Sapium*; *Sebastiania*; *Senna*-Type; *Tabebuia*-Type;
185 *Tapirira*-Type); % Forest taxa (*Alchornea*; *Anadenanthera*; *Hedyosmum*; Moraceae; *Myrsine*; *Sloanea*;
186 *Symplocos*; *Trema*); and % cold-adapted taxa (*Drymis*, *Weinmannia*; *Araucaria*). To assess regional
187 patterns of vegetation variability, a Principal Components Analysis (PCA) was performed using the %
188 Grassland taxa, % Savanna taxa and % Forest taxa from the three cores. Prior to PCA, pollen data were
189 interpolated to every 200 years (only considering non-sterile pollen samples) and square-root
190 transformed.

191 Subsamples of 0.5 cm³ taken every 2 cm were prepared for macro-charcoal analysis by treating
192 them with NaOCl and KOH to concentrate charcoal particles. The subsamples were then sieved through
193 160 µm mesh and analyzed in the microscope to separate charcoal particles. WinSeedle software (Regent
194 Instruments, Quebec, Canada) was used to count the particles and measure their size. Charcoal data are
195 expressed as charcoal influx (number of particles/cm²/year) and as charcoal area (charcoal total
196 area/cm²/year).

197 The entire core was subjected to XRF core scanning with a resolution of 0.5 cm at the *Laboratoire*
198 *EDYTEM Université Savoie Mont-Blanc* - CNRS. Two runs were performed, with the settings of the first run
199 adjusted at 10 kV to measure light elements (Al to Fe), while the settings of the second run were adjusted
200 to 30 KV for heavier elements (Cu to Pb). Titanium, which is considered an unambiguous indicator of
201 allochthonous input (Davies *et al.*, 2015), was used to normalize other elements (Ca, Fe, S, Si, Sr, Zn) and
202 discriminate in-lake mineral input.

203 **4. Results for the Lagoa Feia record**

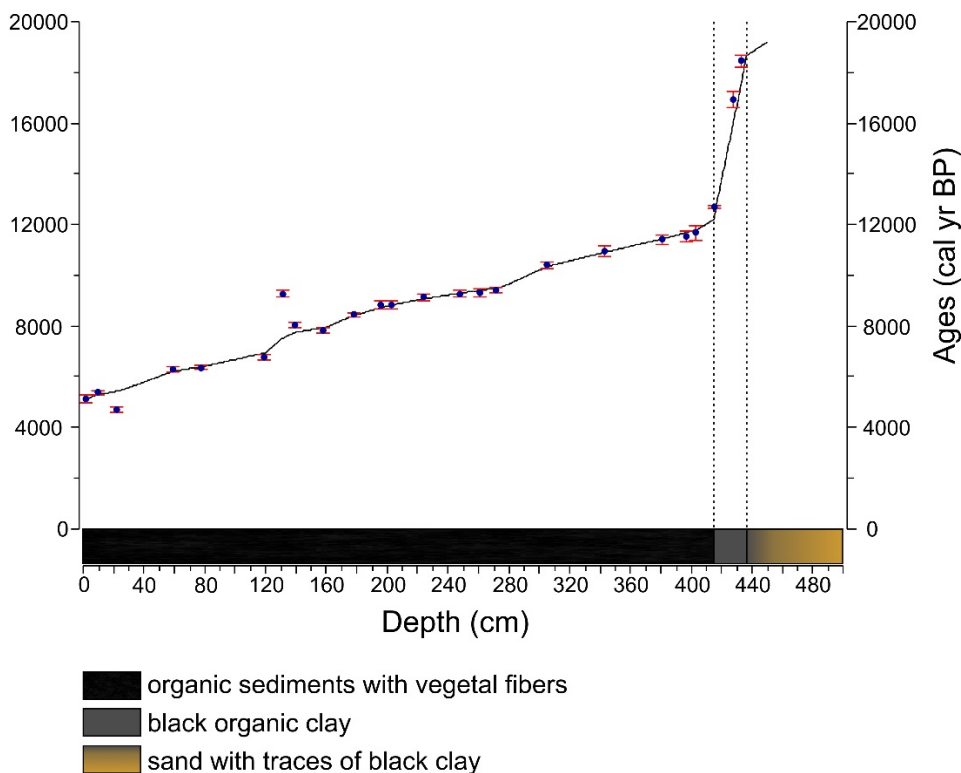
204 *4.1. Core sedimentology, XRF scanning results and chronology*

205 Core LF15-2 demonstrated three distinct sediment layers: the sediment between 500-437cm was
206 composed of fine to coarse siliciclastic sand, with clay content increasing towards the top of the layer; the

207 sediment between 437-415.5 cm was composed of black clay; while the sediment from 415.5 cm to the
 208 top of the core was mainly composed of organic sediment with vegetal fibers (Fig. 2).

209 The XRF core scanning results also revealed three main depositional units that corresponded to
 210 the three sedimentary layers. The XRF scanning results from the bottom to 437 cm indicated high Si
 211 content, along with relatively high K and Al contents (Unit 1, Fig. 3), which reflects the predominance of
 212 siliciclastic sand. The clay layer above this first depositional unit (Unit 2) was characterized by an increase
 213 in several lithogenic minerals (Zr, Rb, K, Al and Ti) as well as Fe and Ca; Si was not as noticeable in this
 214 layer as it was in the bottom layer. The organic layer (spanning from a depth of 415.5 cm to the top (Unit
 215 3)) displayed decreased levels of all lithogenic minerals relative to the other layers, and high levels of S, Ca
 216 and Sr.

217



218
 219 **Figure 2:** Lithology and age-depth model for the LF15-2 sediment core. Calibration intervals for ¹⁴C dates are
 220 plotted in red. Boundaries for accumulation rate calculations were set at the thresholds between different
 221 sediment layers (vertical dashed lines).
 222

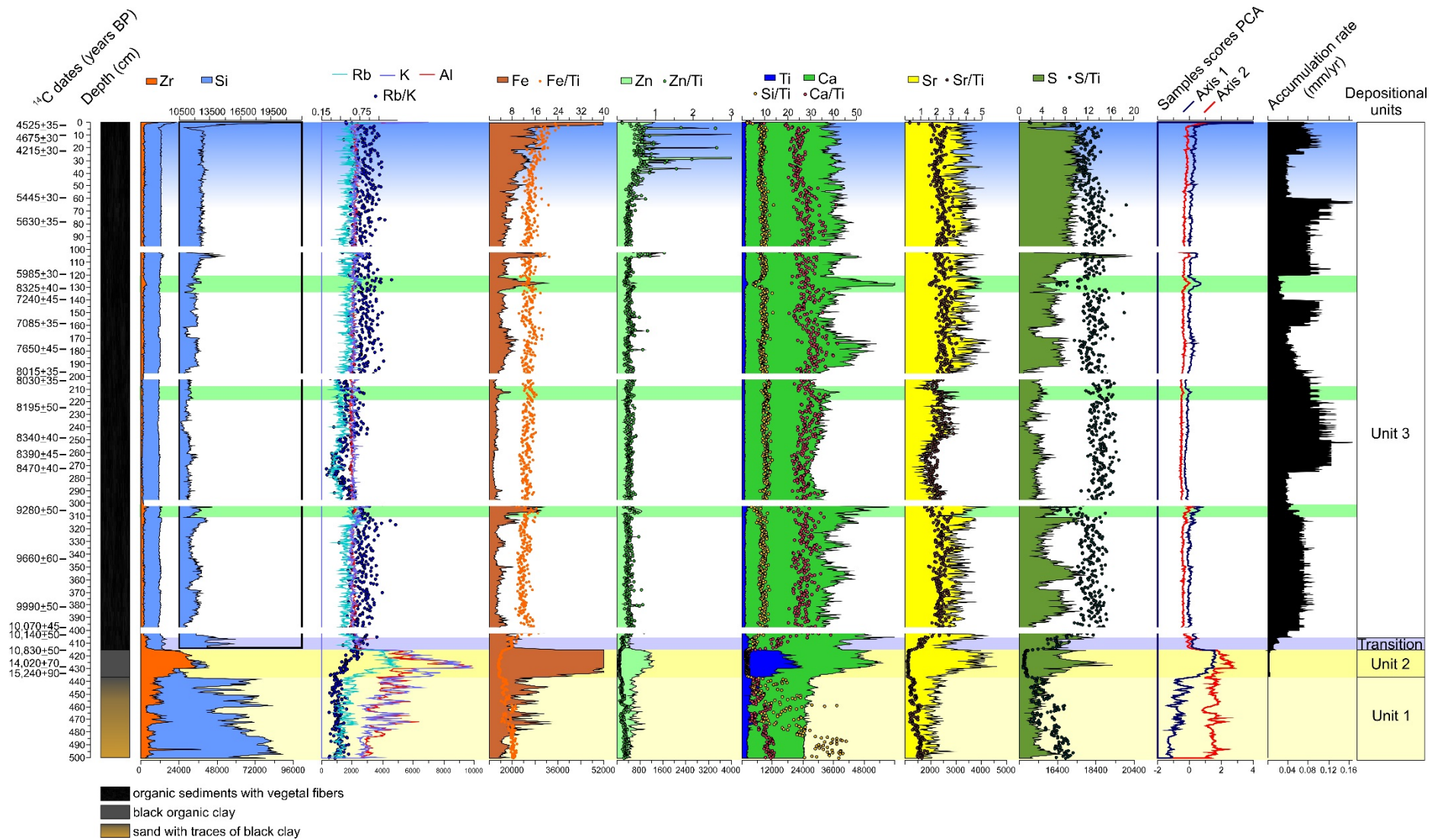
223 These depositional units revealed three different stages of sedimentation in the Lagoa Feia basin.
 224 Unit 1 shows medium to high-energy deposition of detrital sediments, which was most probably related
 225 to alluvial deposition prior to lake formation. Unit 2 reflects conversion to low-energy sedimentation

226 characterized by detrital clay input, which marks the beginning of lacustrine deposition and the drowning
227 of the valley. The low Ca/Ti, Si/Ti and Fe/Ti ratios in unit 2 relative to unit 3 suggest predominantly
228 allochthonous mineral input, without significant contribution of in-lake production. In unit 3, the
229 lacustrine deposition changes to autochthonous organic sedimentation, which explains the low levels of
230 lithogenic elements observed in this unit. Relatively high Ca and Sr levels, along with high Ca/Ti and Sr/Ti
231 ratios, in unit 3 suggest the presence of biogenic/authigenic in-lake carbonate deposition. The transition
232 from unit 2 to unit 3 was gradual, and included a transitional phase during which fine detrital input
233 progressively shifted to organic sedimentation.

234

235

236



237

238 **Figure 3:** XRF scanning results showing the levels of selected elements (Zr, Si, Rb, K, Al, Fe, Zn, Ti, Ca, Sr, S), along with relevant ratios (Rb/K, Fe/Ti, Zn/Ti, Si/Ti, Ca/Ti, S/Ti),
 239 for core LF15-2 plotted against depth. Green bands highlight episodes of increase in Ti and Fe content during Unit 3. Radiocarbon ages are indicated on the left side.

240 Samples scores for the two first axes of the PCA (Supplementary Material, Fig. 1) and accumulation rate curves are shown on the right side. XRF data at the junction of the

241 core sections were disregarded (white bands) because of possible edge-induced errors during the scan.

242

21

22

243 A PCA was performed with the most significant non-organic elements (Supplementary Material, Fig. 1).
244 The PCA was able to differentiate the three main units of sedimentation. The results showed that Ca, Sr, Ni, S and
245 Br were relatively more abundant in the organic sediments of unit 3 than in sediments representing the other
246 units, while lithogenic elements Ti, Si, Zr, K and Al were correlated with samples from units 1 and 2. In unit 3,
247 there were three episodes in which the content of Ti increased (shown by green bands in Fig. 3, and
248 corresponding to decreased Ca/Ti); these episodes were also identified on the first axis of the PCA and could
249 reflect time periods when organic deposition shifted to mineral input. These episodes were also associated with
250 Fe peaks, which suggests that the lake sediments may have been exposed to oxidation as a result of lower lake
251 levels during these periods.

252
253
254 Radiocarbon dates obtained for the upper 435 cm of LF15-2 (Table 1, Fig. 2) show an age of around
255 15,240 ¹⁴C yr BP (~18,400 cal yr BP) at the bottom of the record and 5,525 ¹⁴C yr BP (~5,100 cal yr BP) at the top.
256 The two units with lacustrine deposition (units 2 and 3) showed distinct sedimentation rates on the age-depth
257 curve. The clay layer (unit 2), between 436.5 and 415.5 cm, represents a 4,500 year interval and suggests very low
258 sedimentation rates. The deposition of organic sediments (unit 3) is well constrained by twenty-two radiocarbon
259 dates that indicate higher, and relatively constant, sedimentation rates during the early and middle Holocene. In
260 the LF15-2 age-depth model (Fig. 2), boundaries constraining changes in the sedimentation rate were set at 415
261 and 437 cm to coincide with sedimentological changes.

262 **Table 01:** Radiocarbon dates of the LF15-2 core. Calibrated ages (two standard deviations (2σ) ranges) were obtained
263 from Calib 7.0 (Reimer *et al.*, 2013).

Lab Code	Depth (cm)	¹⁴ C yr BP	δ ¹³ C	Age range (cal yr BP) 2σ
SacA47388	2	4525 ± 35	-26,8	4,976 - 5,297
SacA57452	10	4675 ± 30		5,300 - 5,467
SacA49368	22	4215 ± 30	-31,1	4,582 - 4,834
SacA49369	59	5545 ± 30	-25,2	6,215 - 6,397
SacA47389	78	5630 ± 35	-32	6,298 - 6,441
SacA49373	119	5985 ± 30	-25,7	6,673 - 6,879
SacA57453	131	8325 ± 40		9,131 - 9,426
SacA47393	139	7240 ± 45	-27,6	7,939 - 8,158
SacA49374	158	7085 ± 35	-27,7	7,792 - 7,955
SacA47394	178	7650 ± 45	-26,1	8,343 - 8,536
SacA49375	196	8015 ± 35	-27,4	8,651 - 8,996
SacA49370	203	8030 ± 35	-29,9	8,660 - 9,003
SacA47390	224	8195 ± 50	-20,8	9,001 - 9,264
SacA49371	248	8340 ± 40	-29,1	9,137 - 9,432
SacA47391	261	8390 ± 45	-25,4	9,149 - 9,483
SacA49372	272	8470 ± 40	-29,1	9,314 - 9,529
SacA47395	305	9280 ± 50	-25,9	10,255 - 10,552
SacA47396	343	9660 ± 60	-21,6	10,756 - 11178
SacA48900	381	9990 ± 50	-29,9	11,239 - 11,613
SacA49376	397	10070 ± 45	-29,5	11,313 - 11,756
SacA47398	403	10140 ± 50	-30	11,397 - 11,958
SacA49377	415	10830 ± 50	-24,4	12,659 - 12,753
SacA47399	428	14020 ± 70		16,640 - 17,224
SacA57454	433	15240 ± 90	-22	18,226 - 18,691

264

265

266

4.2. Pollen and charcoal

267

268

269

270

271

272

273

274

275

276

277

278

279

280

281

A total of 155 pollen types were identified from LF15-2 samples (Table 1, Supplementary Material), plus 12 types of spores and other palynomorphs (algae zygospores, zooclasts, "Tintinomorphs" and leaf spines of *Ceratophyllum*). Pollen analysis was performed on the upper 445 cm of the core, i.e., this analysis included the top of depositional unit 1 and units 2 and 3. Pollen concentrations varied noticeably between the units (Fig. 4). The clay layer (unit 2) was characterized by a low sedimentation rate (around 0.003 mm/yr) and showed very high pollen concentrations (around 100,000 grains/cm³), while most samples from the organic sediments of unit 3 showed comparatively lower pollen concentrations (usually less than 20,000 grains/cm³). This may be explained by the high sedimentation rate of unit 3 (maximum of 0.16mm/yr).

A cluster analysis that included terrestrial pollen types identified five pollen zones (Fig. 4):

i) *Zone LF01 (445-421 cm; ca 19,000 to 14,400 cal yr BP; 7 samples)*

This pollen zone corresponds to the top of depositional unit 1 and most of depositional unit 2. Samples showed high frequencies of Poaceae (max. 53%) and marsh plants (*Cuphea* (max. 2.3%), *Xyris* (max. 5%) and *Eryngium* (max. 2%)), as well as high frequencies of Bryophytes (*Phaeoceros* and *Sphagnum*) and *Lycopodiella* (Supplementary Material, Fig. 4). These samples showed relatively low frequencies of Cyperaceae, ferns, and algae. Furthermore, zygospores from *Debarya* were restricted to this zone. Zone LF01 also had high frequencies of

25

26

282 Asteraceae (max. 26.2%), while arboreal forest taxa were represented by *Hedyosmum* (max. 4.9%), *Ilex* (max.
283 2.9%) and *Myrsine* (1.7%). The cold-adapted taxa *Weinmannia* and *Drimys* were also present (Supplementary
284 Material, Fig. 2). Charcoal was not detected from this zone (Fig. 5).

285 ii) Zone LF02 (417-405 cm; ca 13,300 to 11,850 cal yr BP; 4 samples)

286 Zone LF02 corresponds to the transitional zone between depositional units 2 and 3 (Fig. 4), and differs
287 from the previous zone in that it had lower frequencies of Poaceae (< 18%) and marsh plants, and higher
288 frequencies of forest taxa, with the appearance of new arboreal taxa such as *Banisteriopsis*-Type (Malpighiaceae -
289 max. 31%), Moraceae (1%), as well as Annonaceae, *Serjania*, *Prunus* and *Dendropanax* (Supplementary Material,
290 Fig. 2-4). Charcoal was detected from the top of the zone (0.9 particles/cm²/yr) (Fig. 5).

291 iii) Zone LF03 (401-363 cm; 11,800 to 11,190 cal yr BP; 11 samples)

292 This zone showed clear Cyperaceae (72%) and *Blechnum*-Type (88%) peaks. Spores from two other fern
293 genera, *Acrostichum* and *Osmunda*, also showed high frequencies in this zone (Supplementary Material, Fig. 4),
294 while the presence of Bryophytes, *Lycopodiella* and marsh plants has almost disappeared. Aquatic plants
295 (Pontederiaceae) peaked (11%) at around 11,500 cal yr BP, and then become rare. Poaceae showed alternating
296 frequencies, with very high (45%) and low (less than 5%) values. This zone also marks the start of samples with
297 high frequencies of *Gomphrena*. This taxon also shows alternating frequencies, with both high and low values
298 observed throughout the zone. When compared to the previous zone, this zone demonstrates an important
299 change in local vegetation. The forest assemblage observed in the previous zones (comprising *Hedyosmum*, *Ilex*,
300 *Myrsine*, *Banisteriopsis*-Type and *Weinmannia*) shifts to other arboreal forest taxa such as *Anadenanthera* (max.
301 3.6%), Moraceae (max. 14%), *Celtis* (max. 2.4%), and *Doliodocarpus* (max. 4%), as well as *Trema* and *Schefflera*
302 (Supplementary Material, Fig. 4). The arboreal species *Erythrina* (max. 5.8%) was exclusively identified from this
303 zone. Typical Cerrado arboreal taxa *Byrsonima* (max. 4%) and *Astronium*-Type (max. 7.5%) became more
304 abundant in this zone, which also showed isolated presence of *Caryocar*, *Plenckia* and *Forsteronia* (Supplementary
305 Material, Fig. 2-4). Charcoal was present in this zone, although showed low influx (maximum value of 1.8
306 particles/cm²/yr) (Fig. 5).

307 iv) Zone LF04 (359-121 cm; 11,140 to 7,000 cal yr BP; 60 samples)

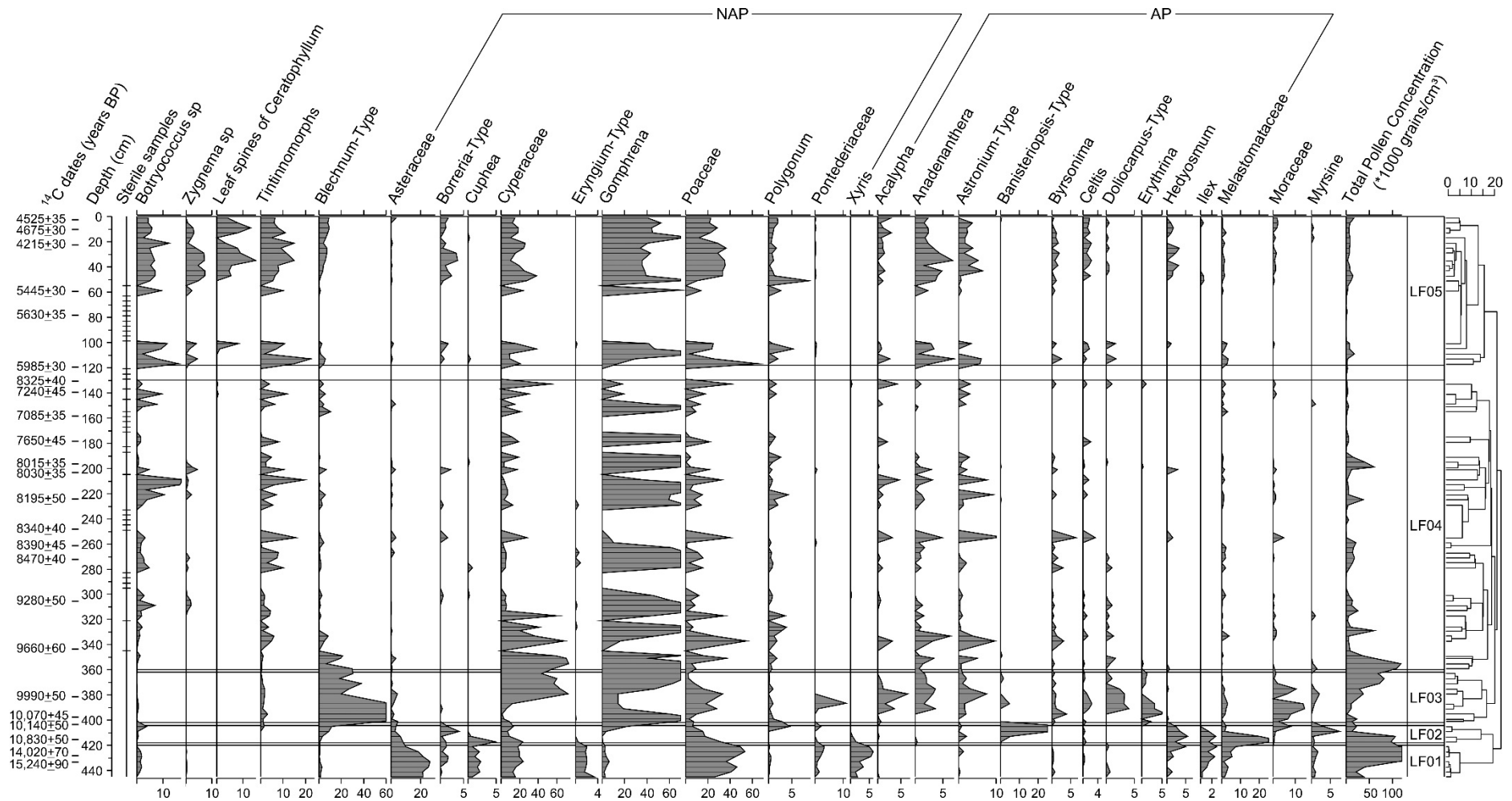
308 Most of the sterile samples identified from the core were concentrated in Zone LF04. These 23 sterile
309 samples were intercalated with 37 pollen-rich samples (more than 20,000 grains/cm³). *Botryococcus*, Cyperaceae,
310 Poaceae and *Gomphrena* showed alternating high and low frequencies throughout the zone. The zone showed
311 lower frequencies of arboreal pollen than the previous zone, and some arboreal forest taxa (e.g. Moraceae,
312 *Doliocarpus*) were either no longer present or had become rare. *Astronium*-Type (0 to 11.3%), *Anadenanthera* (0
313 to 6.4%) and *Byrsonima* (0 to 6%) occurred at irregular frequencies. Two peaks of high charcoal influx were
314 identified from the bottom of this zone, centered at around 11,000 and 10,600 cal yr BP (6.0 and 1.9
315 particles/cm²/yr, respectively) (Fig. 5).

316 v) *Zone LF05 (117-01 cm; 6,900 to 4,980 cal yr BP; 29 samples)*

317 Zone LF05 showed an abundance of *Ceratophyllum* (an aquatic submerged plant) leaf spines (max. 15%)
318 and an increase in the frequency of *Zygnema* zygospore. Furthermore, two aquatic plants that were not observed
319 in the previous zone, *Sagittaria* and Nymphaeaceae, were found in this zone (Supplementary Material, Fig. 2-4).
320 From a depth of 51 cm to the top, the pollen content between samples became less irregular and arboreal taxa
321 such as *Astronium*-Type (max. 6.4%), *Anadenanthera* (max. 6,7%) and *Celtis* (max. 2.3%) showed constant
322 frequencies. Zone LF05 also showed more continuous charcoal influx (Fig. 5), with peaks at 6,750; 6,650 and 5,100
323 cal yr BP (2.3; 1.4 and 5.8 particles/cm²/yr, respectively).

324

325



326
 327 **Figure 4:** Synthetic pollen percentage diagram for the LF15-2 core, with data plotted against depth (y-axis). Radiocarbon dates, positions of sterile samples, the frequency
 328 of 28 selected non-pollen palynomorphs (NPP), non-arboreal pollen (NAP) and arboreal pollen (AP), pollen concentrations, pollen zones and a cluster dendrogram are
 329 shown (from left to right). For a complete diagram, please refer to the Supplementary Materials – Fig. 2-4.

330 **5. Discussion**

331 **5.1. Paleoeological interpretation of the Lagoa Feia record**

332 The observed changes in the geochemical, pollen and charcoal aspects of the Lagoa Feia record describe
333 significant changes in lake, vegetation and fire regime dynamics.

334 Lacustrine deposition at Lagoa Feia began around 19,000 cal yr BP, right after the Last Glacial Maximum
335 (21 to 19 kyr). Lake formation could be explained by local subsidence of the plateau due to sub-superficial
336 limestone dissolution associated with superficial weathering (Ferraz-Vicentini, 1999). These processes would have
337 raised the groundwater table to the surface, which then subsequently drowned the valley and established a
338 source for the downstream Rio Preto river. In Late Pleistocene, until ~13,300 cal yr BP (depositional unit 2 and
339 pollen zone LF01), the very low sedimentation rate of fine sediment and the high content of marsh plants (Fig. 5),
340 Bryophyte and *Lycopodiella* suggest the formation of a shallow lake surrounded by marshes. The high frequencies
341 of Asteraceae and Poaceae indicate an open landscape around Lagoa Feia at that time. The arboreal taxa present
342 in this zone (*Hedyosmum*, *Ilex*, *Myrsine*) are consistent with the presence of gallery forest (Fig. 5). The presence of
343 *Weinmannia* and *Drymis* (Supplementary Material, Fig. 2), which are cold-adapted taxa, along with *Hedyosmum*-
344 *Ilex-Myrsine*, suggests that the climate was colder during this period than it is currently. However, the low
345 sedimentation rates noted for this period, which could also be due to depositional hiatuses, imply that the late
346 Pleistocene is not represented in detail on the Lagoa Feia record.

347 Higher temporal resolution started around 12,300 cal yr BP, which corresponds to a transitional phase
348 towards more organic sedimentation. This change in sedimentation is interpreted to reflect an increase in lake
349 levels. Organic matter originating from algae, ferns and aquatic plants would have been preserved by prevailing
350 anoxic conditions at the lake bottom. The transitional phase detected by XRF scanning corresponds to pollen zone
351 LF02, which showed decreased frequencies of marsh plants and Bryophytes, increased frequencies of *Polygonum*,
352 and the appearance of Tintinomorphs at the top of this zone (Fig. 5). All of these findings are consistent with the
353 transition to a deeper lake environment.

354 Following the transitional phase, a deeper, lacustrine environment is fully established at the beginning of
355 depositional unit 3 (around 11,900 cal yr BP). Cyperaceae and *Gomphrena* (Amaranthaceae) are the most
356 dominant taxa throughout depositional unit 3, and are probably related to local pollen production on the lake

357 margin. Cyperaceae pollen was not differentiated at the genus level, but two types of Cyperaceae pollen were
358 dominant: a smaller pollen type, probably related to *Cyperus*; and a very large pollen type, possibly related to
359 *Eleocharis* (Willard *et al.*, 2004; Pollen collection ISEM). Both genera include amphibious and aquatic plants that
360 colonize bogs, lakes and river margins in the Cerrados (Oliveira *et al.*, 2011). *Gomphrena*, on the other hand, is
361 present in the Cerrados as a herbaceous plant that occurs alongside Poaceae and Cyperaceae on humid or dry
362 soils in open areas (Marchant *et al.*, 2002; Fank-de-Carvalho *et al.*, 2010). The occurrence of fire favors
363 *Gomphrena* seed dispersal and germination (Fank-de-Carvalho *et al.*, 2015), thus these plants tend to proliferate
364 after the passage of fire (Fank-de-Carvalho *et al.*, 2010). Therefore, the predominance of Cyperaceae over
365 *Gomphrena* throughout unit 3 can be interpreted as lacustrine expansion, while samples in which *Gomphrena*
366 frequencies exceeded Cyperaceae frequencies indicate periods characterized by temporary drying of parts of the
367 lake and colonization by herbaceous plants. Although unit 3 represents a rise in lake levels when compared to the
368 previous phase, lake levels were lower than they are now, as well as subject to temporary drying.

369 The increased lake levels observed during the transition to depositional unit 3 also coincide with the
370 development of a more forested landscape. Arboreal pollen was more frequent and diverse in pollen zones LF02
371 and LF03 (i.e. between 12,500 - 11,190 cal yr BP) than in pollen zone LF01, suggesting the expansion of forests
372 and/or arboreal savannas, which were previously limited to streams margins, on the plateau. *Erythrina*, restricted
373 to pollen zone LF03, is associated with a tree that grows on moist habitats and is adapted to periodical flooding
374 (Medina *et al.*, 2009); thus, its presence suggests that a forest was also growing around the lake. Ecological
375 observations of the present-day vegetation of the Cerrados indicate that the degree of arboreal cover is highly
376 influenced by soil moisture. For instance, in a study of the association between Cerrados physiognomies and soil
377 characteristics, Assis *et al.* (2011) showed that soil water availability is the main factor explaining the gradient
378 from open savannas to woodlands when soil fertility is held constant. In another study, Terra *et al.* (2018)
379 analyzed how several environmental factors were linked to the vegetation of 158 sites in Minas Gerais state
380 (central Brazil). Their results demonstrated that soil water availability is the main factor driving tree density in
381 these sites. Therefore, the increase in arboreal cover at Lagoa Feia observed in pollen zones LF02 and LF03 –
382 which are also periods of rising lake levels – could have resulted from increased soil moisture, which is directly
383 influenced by rainfall amount, the main factor underlying groundwater recharge (Cabral *et al.*, 2015). These

384 pollen zones temporally coincide with the Younger Dryas event that can therefore be considered a wet period at
385 the Lagoa Feia site.

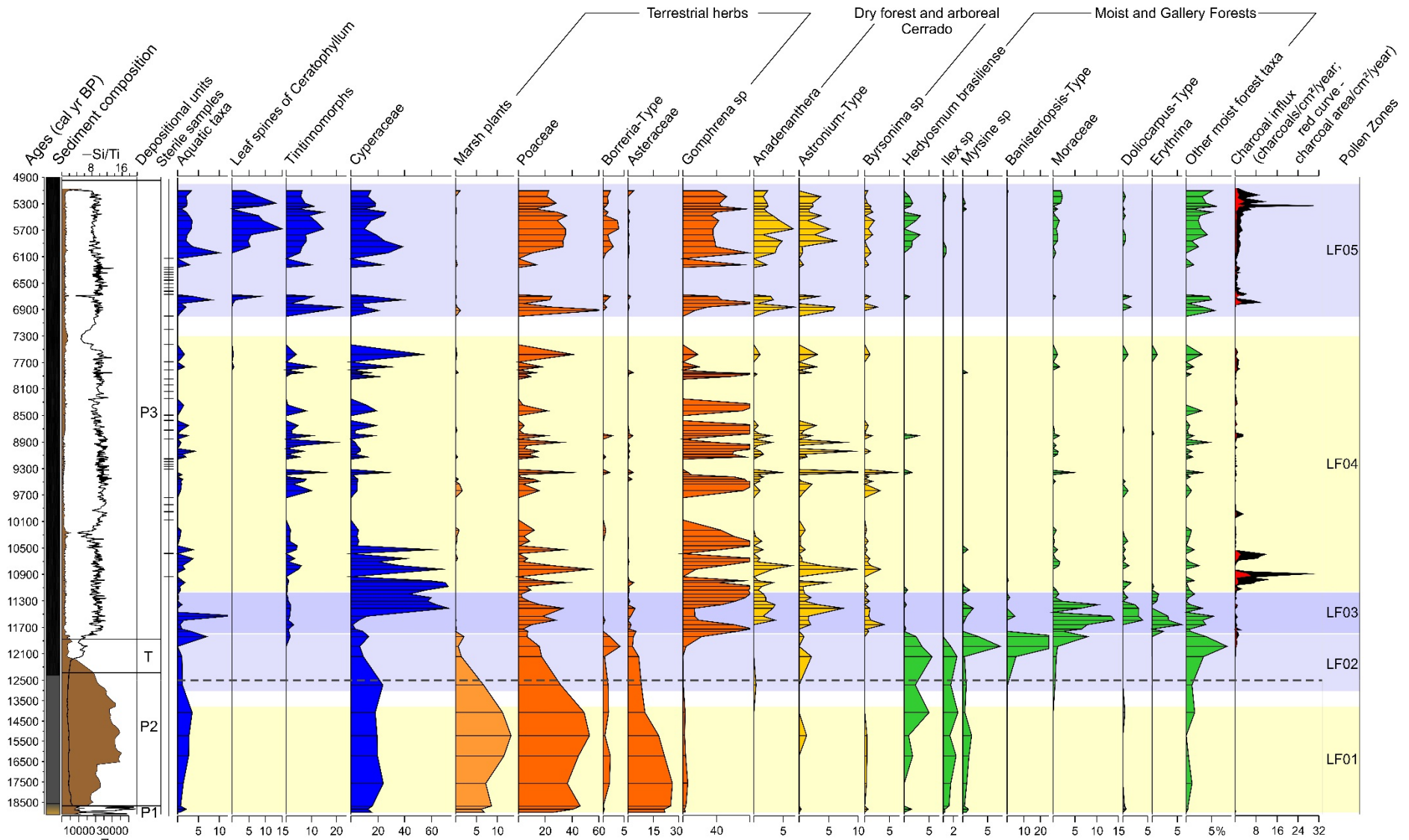
386 From around 11,140 to 7,000 cal yr BP (LF04), gallery and moist forest taxa were less abundant around
387 Lagoa Feia (Fig. 5), suggesting a more open landscape. The discontinuous presence of arboreal Cerrado and dry
388 forest taxa, showed by a succession of high and low frequencies, indicates the repeated growth and decline of
389 arboreal cover. This early Holocene period was also characterized by fluctuations in lake levels, with support
390 coming from the predominance of *Gomphrena* over Cyperaceae, the presence of sterile samples, and episodes of
391 increased mineral input. This suggests that the early Holocene (LF04) was drier than the Younger Dryas (LF02 and
392 LF03), but included a series of centennial-scale moisture oscillations.

393 The onset of these drier conditions coincides with a period of high charcoal influx peaks between 11,000-
394 10,600 cal yr BP (Fig. 5). The occurrence of fires at the beginning of the Holocene might have played a role in the
395 decreasing forest cover observed around Lagoa Feia at that time. Studies based on modern observations suggest
396 that the occurrence of fire significantly influences the degree of arboreal cover in the Cerrados, as frequent fires
397 favor the development of an herbaceous stratum at the expense of a woody layer (Moreira, 2000; Durigan &
398 Ratter, 2016). Fires in the Cerrados are almost exclusively surface fires - crown fires are not common – which burn
399 the aboveground parts of herbs and grasses (Miranda *et al.*, 2010). However, the ashes produced during these
400 fires are deposited on the soil surface, providing nutrients that are readily absorbed by the shallow roots of
401 grasses. As such, fires represent a transfer of nutrients from woody species to grasses (Oliveras *et al.*, 2013).
402 Furthermore, herbaceous species commonly have underground nutrient-storing organs, and the plants transfer
403 nutrients belowground at the beginning of the dry season in a bid to survive fires that can only affect the nutrient-
404 poor aboveground parts (Oliveras *et al.*, 2013). Although some arboreal species of the Cerrados show fire
405 adaptations (Sato *et al.*, 2010), tree recruitment is overall negatively affected by fires (Mistry, 1998).

406 Apart from the peaks at the beginning of zone LF04, charcoal accumulation was not abundant during the
407 early Holocene dry period. The low frequency of fires during this relatively drier phase could be due to a different
408 pattern of annual rainfall distribution. Natural fires in the modern Cerrados are triggered by lightning and occur
409 during the wet season or during the transitional months between seasons (Ramos-Neto & Pivello, 2000; Medeiros
410 & Fiedler, 2004; Fiedler *et al.*, 2006). Although lightning and natural fires were observed to be more frequent

411 during the wet season, these fires are quickly extinguished by subsequent rain and only burn small areas (Ramos-
412 Neto & Pivello, 2000). Natural fires occurring in September, which represents the transition from the dry to the
413 rainy season, burn significantly larger areas because at this time vegetation - which is still affected by the severe
414 water deficit from the dry season – offers plenty of dry fuel (Ramos-Neto & Pivello, 2000); these types of fires
415 have the most significant impact on vegetation (Miranda *et al.*, 2010). The absence of sparse rains during the
416 transition phase between seasons could explain the relatively low occurrence of fires during most of the early
417 Holocene.

418 From around 6,900 to 5,000 cal yr BP, the presence of *Ceratophyllum* and a decrease in *Gomphrena*
419 frequencies suggest relatively higher, and more stable, lake levels. Furthermore, arboreal vegetation
420 representative of both moist and dry forests has a steadier presence around the lake (Fig. 5). Nevertheless, the
421 pollen record suggests that the studied region had less forests in this time period than during the wet period of
422 the Younger Dryas (LF02 and LF03). Pollen zone LF05 demonstrated high charcoal influx with almost all of the
423 samples including charcoal particles and high peaks observed in the beginning and towards the end of the phase.
424 The increased fire occurrence might have been linked to higher fuel availability and/or multiple rain events during
425 the transition between dry and wet seasons. Alternatively, the growing human populations in Central Brazil at the
426 time (Klink & Moreira, 2002) might have played a role in the increased fire frequency.

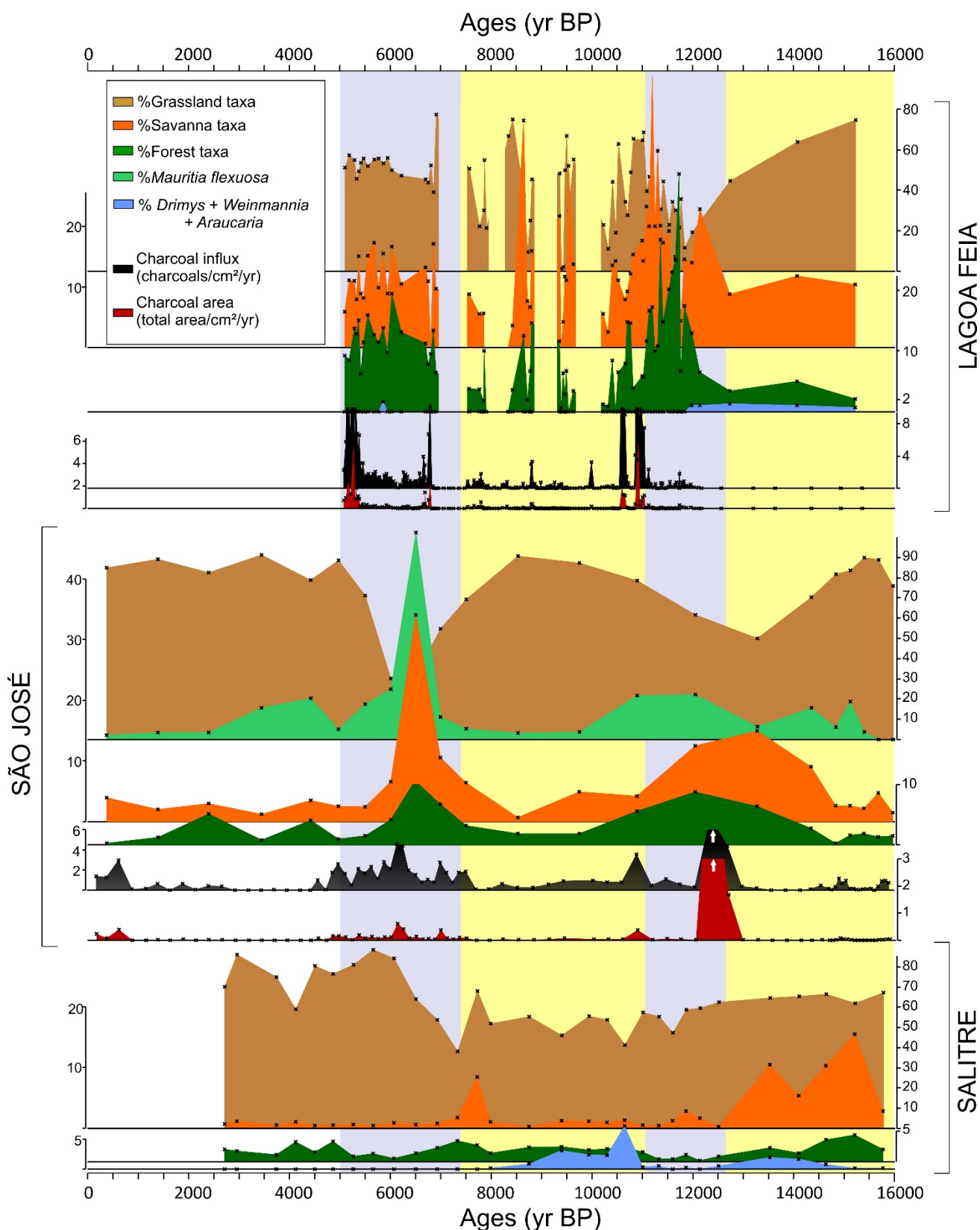


427
 428 **Figure 5:** Summary pollen diagram for the LF15-2 core, with the data plotted against time (cal yr BP). Sediment composition, Zr levels, Si/Ti ratio and depositional phases
 429 are shown on the left. Background colors separate the five pollen zones (shown on the right); light yellow and shades of blue indicate drier and wetter phases, respectively.
 430 The bottom part of the core - below the dashed horizontal line - has a compressed time scale.

431 **5.2. Central Brazilian Cerrados during the Pleistocene-Holocene transition and early Holocene**

432 To test the regional scope of the paleoecological interpretation of the Lagoa Feia record, we compared
433 our results with pollen records from the São José palm swamp (17°04'S, 45°06'W) (Cassino *et al.*, 2018), located
434 around 300 km to the southeast, and the Salitre bog (19°S 46°46'W) (Ledru, 1993), located around 400 km to the
435 south (Fig. 6).

436 The Lagoa Feia and São José sites showed similar trends of vegetation cover and charcoal influx between
437 15 and 5 kyr BP, while the Salitre site for the same period showed an anti-phased trend. Between 12,700 and
438 11,200 cal yr BP, the Lagoa Feia and São José sites showed an increase in forest taxa frequencies, while the Salitre
439 site, which is further south from the other two locations, showed a decrease in the frequencies of forest taxa (Fig.
440 6). São José showed relatively high frequencies of *Mauritia flexuosa* during this time period, which indicates the
441 expansion of the palm swamp. During the early Holocene and beginning of the middle Holocene (~11,200 - 7,300
442 cal yr BP), an opposite trend was observed: at the Lagoa Feia and São José sites, forest taxa and arboreal savanna
443 taxa, as well as *Mauritia flexuosa* at the São José palm swamp, were not as abundant as before, while the Salitre
444 record revealed an increase in forest taxa, including the cold-adapted taxa *Drymis* and *Araucaria*. Subsequently,
445 the Lagoa Feia and São José records showed a general trend of increasing arboreal taxa and *Mauritia flexuosa*
446 frequencies between ~7,000 - 5,000 cal yr BP, while the Salitre site showed generally low forest taxa frequencies
447 during this time period (Fig. 6).



448
 449 **Figure 6:** Synthetic representation of paleoecological changes over the last 16,000 years observed from the Lagoa Feia
 450 (this study), São José and Salitre cores (from Cassino *et al.*, 2018 and Ledru, 1993, respectively). Grassland, savanna and
 451 forest include the following taxa: % Grassland taxa - *Alternanthera*, *Asteraceae*, *Cuphea*, *Drosera*, *Eriocaulaceae*,
 452 *Galianthe*, *Poaceae*, *Xyris*; % Savanna taxa - *Astronium*-Type, *Borreria*-Type, *Byrsonima*, *Caryocar*, *Cupania*, *Forsteronia*-
 453 Type, *Matayba*, *Mimosa*-Type, *Myrtaceae*, *Plenckia*, *Richardia*, *Roupala*, *Sapium*, *Sebastiania*, *Senna*-Type, *Tabebuia*-

454 Type, *Tapirira*-Type; and % Forest taxa - *Alchornea*, *Anadenanthera*, *Hedyosmum*, *Moraceae*, *Myrsine*, *Sloanea*,
 455 *Symplocos*, *Trema*.

456
 457 This opposite trend between sites, i.e. forest expansion at the Lagoa Feia and São José sites synchronic to

458 forest regression at the Salitre site and vice-versa, is visible in the first axis of the Principal Components Analysis of

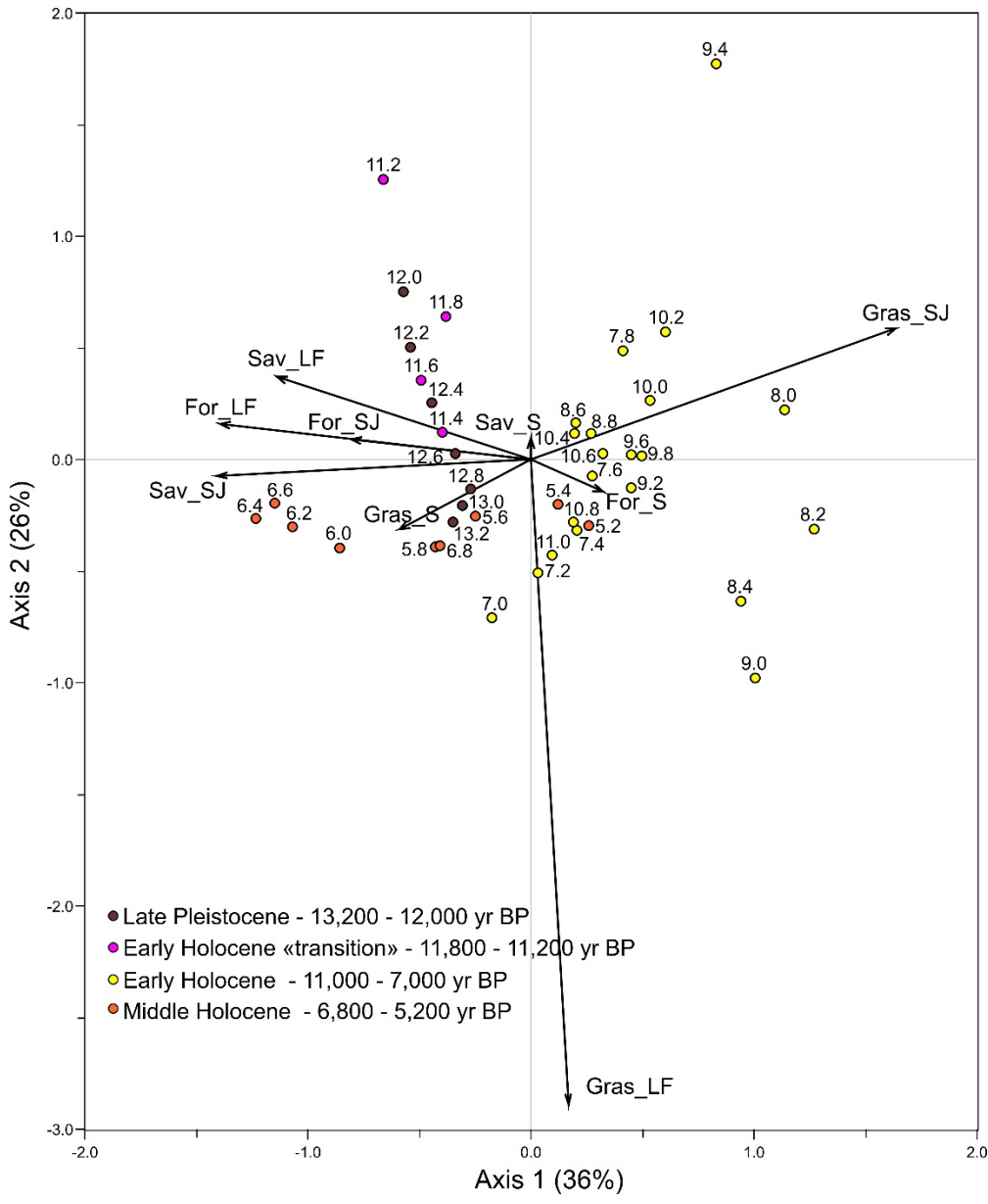
459 interpolated pollen data (PC1; Fig. 7). Time slices in which forest and arboreal savanna frequencies were high at

460 the Lagoa Feia and São José sites and grassland taxa frequency was high at the Salitre site (between 13,200-

461 11,200 cal yr BP and 7,000-5,600 cal yr BP) showed negative PC1 scores. For the early-middle Holocene (~11,000-

462 7,000 cal yr BP), time slices were characterized by high frequencies of forest taxa at the Salitre site and high

463 frequencies of grassland taxa at the Lagoa Feia and São José sites, and showed positive PC1 scores.



464

465 **Figure 7:** Principal Components Analysis of interpolated pollen data from Lagoa Feia, São José and Salitre records.
466 Sample labels refer to ages in kyr BP. Species labels: Gras: % Grassland taxa; For: % Forest taxa; Sav: % Savanna arboreal
467 taxa; LF: Lagoa Feia; S: Salitre; SJ: São José.

468 Charcoal records from Lagoa Feia and São José showed several common trends during the early and
469 middle Holocene (Fig. 6). Peaks of high charcoal influx were detected from both cores at the beginning of the
470 early Holocene, around 11,000 cal yr BP, although this was only detected from one São José sample. The São José
471 record also showed very high charcoal influx around 12,500 cal yr BP, but the charcoal particles in these samples
472 were noticeably larger than the particles from other samples (Fig. 6). This suggests that this peak represents a
473 local fire that had reached the palm swamp border, from where the core was collected. Both records showed
474 relatively low charcoal influx during most of the drier early-middle Holocene (11,000-7,000 cal yr BP), and higher
475 charcoal influx during the relatively wetter middle Holocene (7,000-5,000 cal yr BP). The similarities in vegetation
476 cover and charcoal influx between the Lagoa Feia and São José records support regional climatic control on
477 arboreal cover and fire variability in central Cerrados during the Pleistocene-Holocene transition, while the
478 contrasting trend for vegetation in the Salitre record indicates that different climatic processes affected the
479 southern areas of this region.

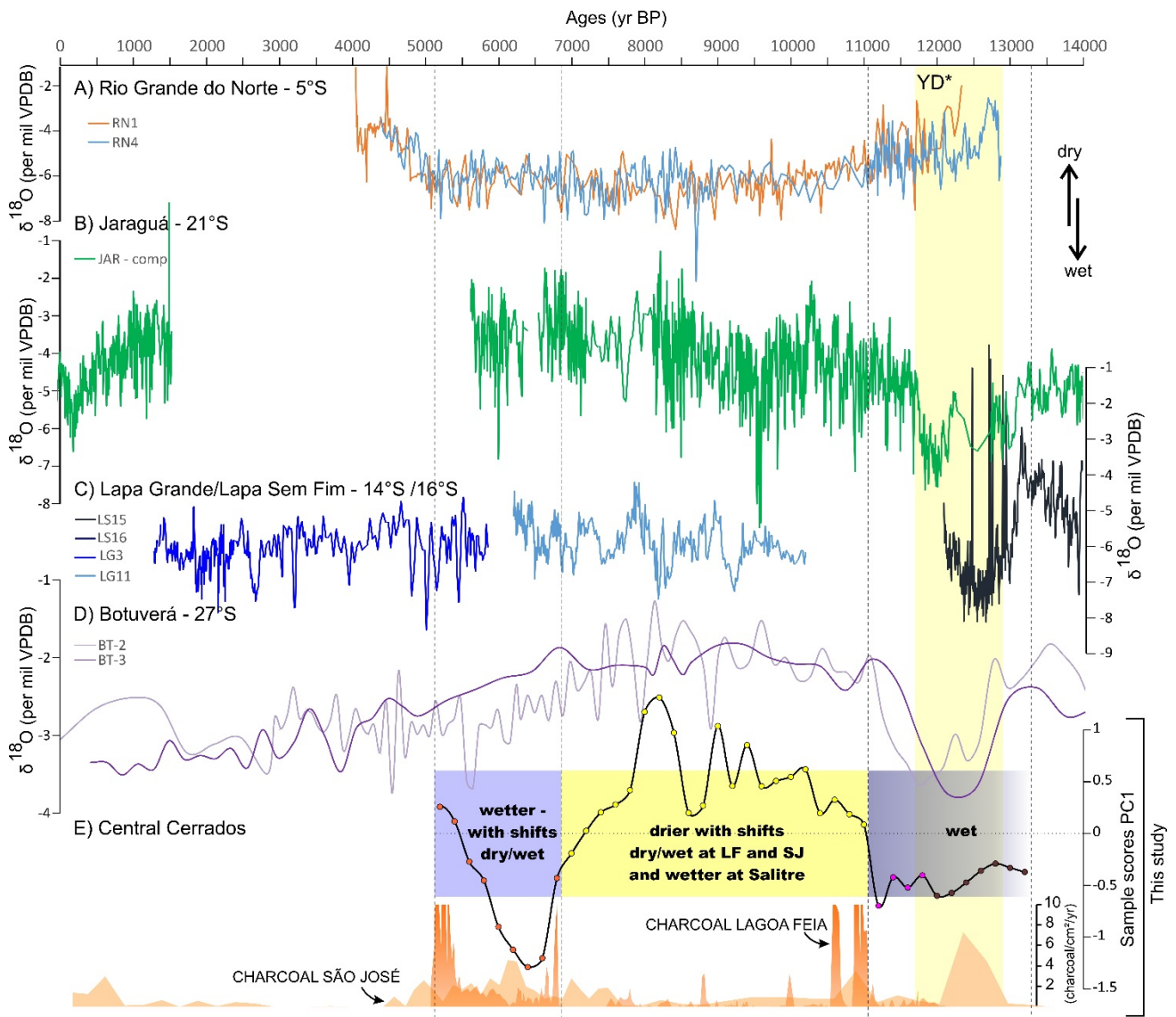
480

481 **5.3. SASM in central Brazil during the Pleistocene-Holocene transition and early Holocene**

482 SASM variability in the central Cerrados during the Pleistocene-Holocene transition and early Holocene
483 can be assessed by comparing vegetation cover variability in the central Cerrados, represented by the PC1 scores
484 (Fig. 7) curve, with $\delta^{18}\text{O}$ speleothem records from adjacent regions (Fig. 8). During the Younger Dryas event
485 (~13,000-11,200 cal yr BP), increased arboreal cover at Lagoa Feia and São José, shown by the PC1 scores curve
486 and indicative of wetter conditions, correlates with more pronounced SASM activity in southern (Botuverá - Cruz
487 *et al.*, 2005; Wang *et al.*, 2007), central-eastern (Lapa Sem Fim - Stríkis *et al.*, 2015) and central-western (Jaraguá -
488 Novello *et al.*, 2017) Brazil (Fig. 8). This suggests that there was increased monsoon activity over a large area at
489 that time (Fig. 9). The increase of monsoon activity in central South America during the Younger Dryas correlates
490 with a dry episode in Northeastern Brazil (Fig. 8A; Cruz *et al.*, 2009), and in northern South America (Haug *et al.*,
491 2001; Maslin *et al.*, 2011) which can be interpreted as a result of southward shifts in the ITCZ (Lea *et al.*, 2003)
492 and the SACZ (Cruz *et al.*, 2005). Our results show that this area of stronger monsoon activity included central
493 Brazil. This disagrees with previously studied pollen records from the Cerrados region (Salgado-Labouriau *et al.*,

494 1997a; Barberi *et al.*, 2000), in which the lack of deposition was interpreted as continuous aridity from the LGM to
 495 the Holocene. The curve representing vegetation variability in central Cerrados shows some delay in the timing of
 496 the end of this wetter phase in comparison to the $\delta^{18}\text{O}$ records from Jaraguá and Botuverá (Fig. 8B and 8DC);
 497 there is no data for the end of the Younger Dryas in the Lapa Grande/Lapa Sem Fim record (Fig. 8C). This could
 498 reflect either an artefact from the interpolation of low-resolution pollen data or a delayed response (around 200
 499 years) of vegetation to a changing climate.

500



501 **Figure 8:** Comparison of vegetation cover variability in central Cerrados and $\delta^{18}\text{O}$ speleothem records from adjacent
 502 regions. A) $\delta^{18}\text{O}$ speleothem record from Rio Grande do Norte (5°S) (Cruz *et al.*, 2009); B) $\delta^{18}\text{O}$ speleothem record from
 503 Jaraguá (21°S) (Novello *et al.*, 2017); C) $\delta^{18}\text{O}$ speleothem records from Lapa Grande (14°S)/Lapa Sem Fim (16°S) (Strikis
 504 *et al.*, 2011; 2015); D) $\delta^{18}\text{O}$ speleothem records from Botuverá (27°S) (Cruz *et al.*, 2005; Wang *et al.*, 2007); E) PC1
 505 scores curve representing vegetation trends in central Cerrados, along with climatic significance and charcoal influx for
 506 Lagoa Feia (LF) and São José (SJ). $\delta^{18}\text{O}$ data are available at the SISAL database (Atsawawaranunt *et al.*, 2019). *The age
 507 limits of the global Younger Dryas (YD) event (beige background) are based on Broecker *et al.* (2010).
 508
 509

510 During the early-middle Holocene (~11,000 to 7,000 cal yr BP), the PC1 curve reflecting vegetation
511 variability in the Central Cerrados demonstrates relatively dry conditions at Lagoa Feia and São José, anti-phased
512 with wetter/colder conditions at Salitre. The Lagoa Feia record indicates that this early-middle Holocene dryness
513 in northern central Cerrados was related to the repeated occurrence of dry events, interspersed with wetter
514 events, during a period of weakened SASM activity. This agrees with the abrupt centennial-scale variations in
515 precipitation detected on the Lapa Grande/Lapa Sem Fim and Jaraguá δO^{18} records during the Holocene (Stríkis *et*
516 *al.*, 2011; Novello *et al.*, 2017). The δO^{18} record from Botuverá, in southern Brazil, also showed drier conditions
517 during this period, and these conditions could also be attributed to weaker SASM (Fig. 8). Wet and dry episodes
518 are not synchronous in the δO^{18} records, which may reflect repeated shifts in the southern boundary belt of the
519 SASM during the early Holocene along with effects from northward polar advection. For instance, a dry event
520 centered around 7,800 cal yr BP in Lapa Grande (Stríkis *et al.*, 2011) coincides with a wet event in the Botuverá
521 record, suggesting a southward displacement of the SASM belt at that time.

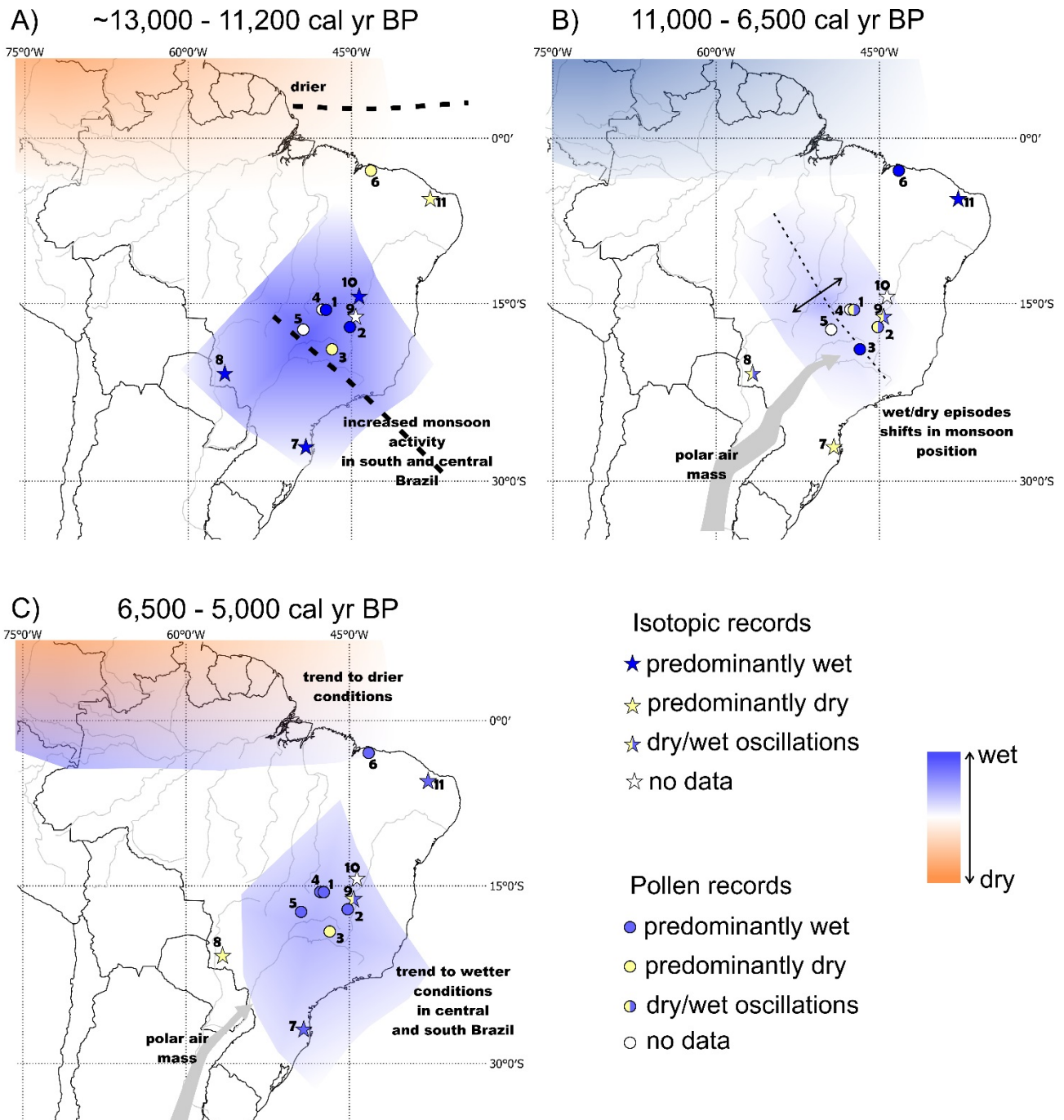
522 The interplay between these repeated shifts in the southern boundary belt of the SASM with the
523 northward polar advection could explain the anti-phase between São José/Lagoa Feia and Salitre. Weaker SASM
524 activity would have allowed frequent and intense polar mass activity at Salitre (Fig. 9), resulting in the
525 development of a moist forest including a mixture of tropical and cold-adapted taxa (Ledru, 1993). Polar air
526 masses have two dominant northward trajectories in southern Brazil: one follows the Atlantic coast and the other
527 penetrates the continent through the Paraná River valley (Boin, 2005). Modern observations have shown that
528 years characterized by weakened tropical Atlantic air mass activity offer less resistance to polar fronts. Hence,
529 during these years the polar fronts can penetrate deep into the Paraná River valley, causing climatic instability
530 and rains in southern and southeastern Brazil (Boin, 2005). Although Salitre is located only 300 and 400 km from
531 São José and Lagoa Feia, respectively, the current vegetation (savanna at Lagoa Feia and São José, and Atlantic
532 semi-deciduous forest at Salitre) shows that the higher altitude and topographic setting of Salitre, located in the
533 highlands bordering the upper Paraná River, cause it to be more affected by polar mass activity. In fact, as the air
534 masses move northward through the Paraná valley they are blocked by the highlands at the upper portion of the
535 valley. As a result, winter rains frequently occur in this area, but the precipitation does not reach the more central
536 regions of the Brazilian highlands where São José and Lagoa Feia are located (Vera et al 2006).

537 The occurrence of sedimentary or pollen hiatuses during the Pleistocene-Holocene transition and early
538 Holocene in the other two previously studied pollen records in Central Cerrados, namely, Cromínia (Salgado-
539 Labouriau *et al.*, 1997a) and Águas Emendadas (Barberi *et al.*, 2000), is likely a consequence of the dry conditions
540 during the early Holocene. Both of these records (Cromínia and Águas Emendadas) were collected from palm
541 swamps, which are shallow depositional sites that are more vulnerable to total drying and erosion than sites like
542 Lagoa Feia. A lake environment was present at the Lagoa Feia site throughout the early Holocene, although it was
543 prone to seasonal temporary dryness. The presence of early Holocene sediments with preserved pollen in the
544 Lagoa Feia record proves that a total desertification of the central Cerrados did not occur in the Holocene period,
545 and that arboreal savanna was part of the landscape even during drier phases. The continuity of a moist
546 depositional environment during the early Holocene at Lagoa Feia has also allowed the preservation of older
547 sediments and provided insight into time periods for which data could not be obtained from other Cerrados sites,
548 i.e., the Younger Dryas wet event. Therefore, the aridification trend that was previously presented for the central
549 Cerrados based on paleoecological records actually corresponds to shifts between dry and wet episodes during
550 the early Holocene (Fig. 9).

551 Between ~6,500-5,200 cal yr BP, central Cerrados pollen records show a trend towards relatively wet
552 conditions, e.g., expansion of the São José palm swamp, increasing lake levels at Lagoa Feia, and a re-expansion of
553 the palm swamps at Cromínia (Salgado-Labouriau *et al.*, 1997a) and Águas Emendadas (Barberi *et al.*, 2000).
554 These data indicate that moisture supply from SASM activity became more regular than it had been during the
555 early Holocene, although the climate at this time period was still relatively drier than it is currently (Prado *et al.*,
556 2013). A reconstruction of local moisture from the $^{87}\text{Sr}/^{86}\text{Sr}$ speleothem record of Tamboril cave, located around
557 60 km south of Lagoa Feia in central Brazil, disagrees with this trend, as the record indicated drier conditions from
558 around 6,000 to 2,000 cal yr BP relative to a wetter early Holocene (Ward *et al.*, 2019). However, this finding
559 might reflect different local conditions of the Tamboril cave, as most sites in central Brazil show a trend of
560 increasing humidity from the middle Holocene onwards. This trend also coincides with wetter conditions in the
561 Botuverá δO^{18} record from southern Brazil, and can be linked to stronger SASM activity and increasing summer
562 insolation in the SH from the middle Holocene to the present (Cruz *et al.*, 2005; Ward *et al.*, 2019). The Lapa
563 Grande/Lapa Sem Fim δO^{18} record is not continuous in the middle Holocene, but showed a strong wet event

564 centered at around 5,200 cal yr BP (Stríkis *et al.*, 2011). Increasing SASM activity in southern and central Brazil
 565 from the middle Holocene onwards is correlated with increasing dryness in northern South America (Haug *et al.*,
 566 2001) and northeastern Brazil (De Oliveira *et al.*, 1999; Cruz *et al.*, 2009) starting around 6,000 - 5,000 cal yr BP.
 567 This trend reflects the interplay between the southward displacement of the ITCZ, increased convection in central
 568 South America and enhanced subsidence in northeastern Brazil.

569



570 **Figure 9:** Schematic representation of SASM position and activity during the Pleistocene-Holocene transition and early-
 571 middle Holocene in central Cerrados. A) ~13,000 to 11,200 cal yr BP; B) 11,000 to 6,500 cl yr BP; C) 6,500 to 5,000 cal yr
 572 BP. Pollen sites: 1. Lagoa Feia (this study); 2. São José (Cassino *et al.*, 2018); 3. Salitre (Ledru, 1993; Ledru *et al.*, 1996);
 573

574 4. Águas Emendadas (Barberi *et al.*, 2000); 5. Cromínia (Salgado-Labouriau *et al.*, 1997a); 6. Caçó (Ledru *et al.*, 2006).
575 Speleothem records: 7. Botuverá (Cruz *et al.*, 2005; Wang *et al.*, 2007) ; 8. Jaraguá (Novello *et al.*, 2017) ; 9. Lapa Grande
576 (Stríkis *et al.*, 2011 ; Stríkis *et al.*, 2015); 10. Lapa Sem Fim (Stríkis *et al.*, 2015); 11. Rio Grande do Norte (Cruz *et al.*,
577 2009). Trends for northern South America are based on research from Haug *et al.*, 2001 and Maslin *et al.*, 2011.

578
579 Similar trends in charcoal influx between the Lagoa Feia and São José sites suggest a link between fire
580 activity and SASM variability. During the wet Younger Dryas, charcoal was not abundant in the Lagoa Feia and São
581 José records, with the exception of one peak of large charcoal particles in the São José record that could be
582 related to a single local fire. Fire activity increased at both sites around 10,800 cal yr BP following the onset of
583 drier conditions during the early Holocene. The decreased SASM activity in central Brazil and the subsequent
584 longer, more severe dry season, along with the high fuel availability inherited from the previous wet period, is
585 likely to have triggered this increase in fire activity. The intense fire activity corresponded to a decrease in
586 arboreal cover at Lagoa Feia, which suggests that fire plays an important role in vegetation turnover across the
587 central Cerrados. This contrasts with results obtained from Laguna La Gaiba (Power *et al.*, 2016), which lies in the
588 transition between seasonally dry tropical forests and Pantanal on the border between Bolivia and Brazil. The
589 Laguna La Gaiba record also suggests a drier early-middle Holocene, but with a different timing compared to the
590 central Cerrados: dryness appeared between 10,000-4,000 cal yr BP and was related to changes in forest
591 composition. However, the charcoal record from Laguna La Gaiba shows an intensification of fire activity around
592 7,500 cal yr BP, approximately two millennia after the onset of drier conditions, and this intensification of fire was
593 not correlated with a change in vegetation. Hence, data from Laguna La Gaiba suggest that fire had a limited
594 influence on vegetation at that site (Power *et al.*, 2016), which contrasts with our results for the Cerrados.

595 6. Conclusions

596 The Pleistocene-Holocene transition and early Holocene are characterized by a succession of wet and dry
597 episodes related to shifts in the SASM boundary belt. These shifts in rainfall distribution affected biodiversity,
598 vegetation structure and fire activity in the central Cerrados.

599 During the last 13 kyr, three main phases were identified from pollen records from central Brazil. The first
600 phase, between 13,000 and 11,200 cal yr BP, showed noticeably increased SASM activity in central Brazil, which
601 was linked to a forested landscape and low fire activity. This finding agreed with speleothem records from
602 latitudes between 15° to 27°S. The next phase, which occurred during the early-middle Holocene, was
603 characterized by centennial-scale oscillations between dry and wet episodes, which caused alternating expansion

604 and regression phases of arboreal cover and lake levels at Lagoa Feia. The SASM belt shifted significantly, and
605 multiple times, in the central Cerrados between 11,200 and 6,500 cal yr BP, and the presented findings suggest
606 that these oscillations intensified the influence of polar air masses in the interior of southeastern Brazil. Fire
607 activity increased for a short period right after 11,000 cal yr BP in the central Cerrados, which coincided with the
608 identified decrease in arboreal cover, and then decreased during most of the early Holocene. During the final
609 distinct phase, between ~ 6,500 and 5,000 cal yr BP, climate conditions in the central Cerrados were relatively
610 wetter than what had been witnessed during the early Holocene, but drier than modern conditions.

611 **Acknowledgements**

612 This work was supported by UMR ISEM and IRD and is part of the projects - Dimensions of biodiversity FAPESP
613 (BIOTA 444 2013/50297-0), NSF (DEB 1343578) and NASA, and the Labex-CEBA. We thank Anne-Lise Develle at
614 the Laboratoire Environnement Dynamique Territoire Montagne (EDYTEM) (University of Savoie, CNRS) for her
615 assistance in the XRF scanning analyses, Vania Pivello (Ib-USP) for her assistance in the fieldwork, Boromir
616 Bogumil for filming the fieldwork at Lagoa Feia (film available at: [https://www.youtube.com/watch?
617 v=sz3zV7QC_H0](https://www.youtube.com/watch?v=sz3zV7QC_H0)), and Paulo de Oliveira (USP) for lending us the corer and boats used to core at Lagoa Feia.

618

619 **Bibliography**

- 620 Alvares, C.A., Stape, J.L., Sentelhas, P.C., Gonçalves, J.L.M., Sparovek, G. 2013. Köppen's climate
621 classification map for Brazil. *Meteorologische Zeitschrift*. 22(6), 711-728. doi:10.1127/0941-2948/2013/0507
- 622 Assis, A.C., Coelho, R.M., Pinheiro, E.S., Durigan, G. 2010. Water availability determines
623 physiognomic gradient in an area of low-fertility soils under Cerrado vegetation. *Plant Ecology*. 212, 1135-
624 1147. DOI 10.1007/s11258-010-9893-8
- 625 Atsawawaranunt, K., Harrison, S., Comas-Bru, L. 2019. SISAL (Speleothem Isotopes Synthesis and
626 AnaLysis Working Group) database version 1b. Dataset. University of Reading, Reading, United Kingdom.
627 <http://dx.doi.org/10.17864/1947.189>
- 628 Barberi, M., Salgado-Labouriau, M.L., Suguio, K. 2000. Paleovegetation and paleoclimate of “Vereda
629 de Águas Emendadas”, central Brazil. *Journal of South American Earth Sciences*. 13, 41-254.
630 [https://doi.org/10.1016/S0895-9811\(00\)00022-5](https://doi.org/10.1016/S0895-9811(00)00022-5).
- 631 Bennett, K.D., Willis, K.J. 2001. Pollen. In: Smol, J.P., Birks, H.J.B., Last, W.M. (Eds.) *Tracking
632 Environmental Change Using Lake Sediments*, Vol. 3, Terrestrial, Algal, and Siliceous Indicators. Kluwer
633 Academic Publishers, Dordrecht, Netherlands, p. 5-32.
- 634 Blaauw, M., Christen, J.A. 2011. Flexible paleoclimate age-depth models using an autoregressive
635 gamma process. *Bayesian Analysis*. 6(3), 457-474. DOI:10.1214/11-BA618
- 636 Boin, M.N., Zavattini, J.A. 2005. Variações do ritmo pluvial no oeste paulista: gênese e impactos
637 erosivos. *Geografia*. 30(1), 115-139.

638 Broecker, W.S., Denton, G.H., Edwards, R.L., Cheng, H., Alley, R.B., Putnam, A.E. 2010. Putting the
639 Younger Dryas cold event into context. *Quaternary Science Reviews*. 29(9-10), 1078-1081.
640 <https://doi.org/10.1016/j.quascirev.2010.02.019>.

641 Cabral, O.M.R., Da Rocha, H.R., Gash, J.H., Freitas, H.C., Ligo, M.A.V. 2015. Water and energy fluxes
642 from a woodland savanna (cerrado) in southeast Brazil. *Journal of Hydrology: Regional Studies*. 4, 22-40,
643 <https://doi.org/10.1016/j.ejrh.2015.04.010>.

644 Cassino, R.F., Martinho, C.T., Caminha, S.A.F.S. 2018. A Late Quaternary palynological record of a
645 palm swamp in the Cerrado of central Brazil interpreted using modern analog data. *Palaeogeography,*
646 *Palaeoclimatology, Palaeoecology*. 490, 1-16. [10.1016/j.palaeo.2017.08.036](https://doi.org/10.1016/j.palaeo.2017.08.036).

647 Cheng, H., Fleitmann, D., Edwards, L.R., Wang, X., Cruz, F.W., Auler, A.S., Mangini, A., Wang, Y., Kong,
648 X., Burns, S.J., Matter, A. 2009. Timing and structure of the 8.2 kyr B.P. event inferred from $\delta^{18}\text{O}$ records of
649 stalagmites from China, Oman, and Brazil. *Geology*. 37, 1007-1010. doi:10.1130/G30126A.1.

650 Cheng, H., Sinha, A., Cruz, F.W.J., Wang, X., Edwards, R.L., D'horta, F.M., Ribas, C.C., Vuille, M., Stott,
651 L.D., Auler, A.S. 2013. Climate change patterns in Amazonia and biodiversity. *Nature Communications*. 4, 1-6.
652 doi:10.1038/ncomms2415

653 Cruz, F.W.J., Burns, S.J., Karmann, I., Sharp, W.D., Vuille, M., Cardoso, A.O., Ferrari, J.A., Silva Dias,
654 P.L., Viana, O. 2005. Insolation-driven changes in atmospheric circulation over the past 116,000 years in
655 subtropical Brazil. *Nature*. 434(7029), 63-66. doi:10.1038/nature03365

656 Davies, S.J., Lamb, H.F., Roberts, S.J. 2015. Micro-XRF core scanning in palaeolimnology: recent
657 developments. In: Croudace, I.W., Rothwell, R.G. (Eds.) *Micro-XRF studies of sediment cores: Applications of*
658 *a non-destructive tool for the environmental sciences*. Developments in Paleoenvironmental Research, 17,
659 Springer, Dordrecht, Netherlands, p. 189-226. DOI 10.1007/978-94-017-9849-5_7

660 De Oliveira, A.L.R., Gil, A.S.B, Bove, C.P. 2011. Hydrophytic Cyperaceae from the Araguaia river basin,
661 Brazil. *Rodriguésia*. 62(4), 847-866. <http://dx.doi.org/10.1590/S2175-78602011000400012>

662 De Oliveira, P.E., Barreto A.M.F., Suguio K. 1999. Late Pleistocene/Holocene climatic and
663 vegetational history of the Brazilian Caatinga: the fossil dunes of the middle São Francisco River.
664 *Paleogeography, Palaeoclimatology, Paleoeecology*. 152, 319-337. [https://doi.org/10.1016/S0031-](https://doi.org/10.1016/S0031-0182(99)00061-9)
665 [0182\(99\)00061-9](https://doi.org/10.1016/S0031-0182(99)00061-9)

666 Durigan, G., Ratter, J.A. 2016. The need for a consistent fire policy for Cerrado conservation. *Journal*
667 *of Applied Ecology*. 53, 11-15. <https://doi.org/10.1111/1365-2664.12559>

668 Fank-De-Carvalho, S.M., Marchioretto, M.S., Bão, S.N. 2010. Anatomia foliar, morfologia e aspectos
669 ecológicos das espécies da família Amaranthaceae da Reserva Particular do Patrimônio Natural Cara Preta,
670 em Alto Paraíso, GO, Brasil. *Biota Neotropica*. 10, 77-86. [http://dx.doi.org/10.1590/S1676-](http://dx.doi.org/10.1590/S1676-06032010000400011)
671 [06032010000400011](http://dx.doi.org/10.1590/S1676-06032010000400011).

672 Fank-De-Carvalho, S.M., Somavilla, N.S., Marchioretto, M.S., Bão, S.N. 2015. Plant Structure in the
673 Brazilian Neotropical Savannah Species. In: Lo, Y-H., Blanco, J.A., Roy, S. (Eds.) *Biodiversity in Ecosystems -*
674 *Linking Structure and Function*. InTech, London, United Kingdom, p. 407-442. DOI: 10.5772/59066.

675 Ferraz-Vicentini, K. 1999. *História do fogo no Cerrado: uma análise palinológica*. Unpublished PhD
676 Thesis. Departamento de Ecologia, Universidade de Brasília, Brasília, Brazil.

677 Fick, S.E., Hijmanns, R.J. 2017. Worldclim 2: New 1-km spatial resolution climate surfaces for global
678 land areas. *International Journal of Climatology*. 37, 4302-4315. <https://doi.org/10.1002/joc.5086>

679 Fiedler, N.C., Merlo, D.A., Medeiros, M.B. 2006. Ocorrência de incêndios florestais no Parque
680 Nacional da Chapada dos Veadeiros. *Ciência Florestal*. 16, 153-161.
681 <http://dx.doi.org/10.5902/198050981896>

682 Furley, P.A. 1999. The nature and diversity of neotropical savanna vegetation with particular
683 reference to the Brazilian Cerrados. *Global Ecology and Biogeography*. 8, 223-241.
684 <https://doi.org/10.1046/j.1466-822X.1999.00142.x>

685 Gosling, W., Mayle, F.E., Tate, N.J., Killeen, T.J. 2009. Differentiation between Neotropical rainforest,
686 dry forest, and savannah ecosystems by their modern pollen spectra and implications for the fossil pollen
687 record. *Review of Palaeobotany and Palynology*. 153, 70-85. 10.1016/j.revpalbo.2008.06.007

688 Haug, G.H., Hughen, K.A., Sigman, D.M., Peterson, L.C., Röhl, U. 2001. Southward Migration of the
689 Intertropical Convergence Zone through the Holocene. *Science*. 293(5533), 1304-1308. DOI:
690 10.1126/science.1059725

691 Hoffmann, W.A., Moreira, A.G. 2002. The Role Of Fire In Population Dynamics Of Woody. In: Oliveira,
692 P.S., Marquis, R.J. (Eds.). *The cerrados of Brazil: ecology and natural history of a neotropical savanna*.
693 Columbia University Press, New York, p. 159-177. DOI: 10.7312/oliv12042

694 Hogg, A., Hua, Q., Blackwell, P., Niu, M., Buck, C., Guilderson, T., Heaton, T., Palmer, J., Reimer, P.,
695 Reimer, R., Turney, C., Zimmerman, S. 2013. SHCal13 Southern Hemisphere Calibration, 0–50,000 Years cal
696 BP. *Radiocarbon*. 55(4), 1889-1903. DOI: 10.2458/azu_js_rc.55.16783

697 IBGE. 2002. Climate map of Brazil, scale 1:500000, Instituto Brasileiro de Geografia e Estatística, Rio
698 de Janeiro, Brazil.

699 IBGE. 2004. Map of Brazilian biomes, scale 1:500000, Instituto Brasileiro de Geografia e Estatística,
700 Rio de Janeiro, Brazil.

701 Juggins, S. 2007. C2 Version 1.5 User guide. Software for ecological and palaeoecological data
702 analysis and visualisation. Newcastle University, Newcastle upon Tyne, United Kingdom, 73pp.

703 Klink, C.A., Moreira, A.G. 2002. Past and current human occupation, and land use. In: Oliveira, P.S.,
704 Marquis, R.J. (Ed.). *The Cerrados of Brazil: Ecology and Natural History of a Neotropical Savanna*. Columbia
705 University Press, New York, p. 69-88. DOI: 10.7312/oliv12042

706 Kutzbach, J.E, Liu, X., Liu, Z., Chen, G. 2008. Simulation of the evolutionary response of global
707 summer monsoons to orbital forcing over the past 280,000 years. *Climate Dynamics*. 30, 567-579. doi:
708 10.1007/s00382-007-0308-z

709 Lacerda Filho, J.V., Rezende, A., Da Silva, A. (Ed.) 2000. Programa Levantamentos Geológicos Básicos
710 do Brasil. Geologia e Recursos Minerais do Estado de Goiás e do Distrito Federal, Scale 1:500.000, CPRM,
711 Goiânia, Brazil.

712 Lea, D.W., Pak, D.K., Peterson, L.C., Hughen, K.A. 2003. Synchronicity of Tropical and High-Latitude
713 Atlantic Temperatures over the Last Glacial Termination. *Science*. 301, 1361-1364 DOI:
714 10.1126/science.1088470

715 Ledru, M.-P. 1993. Late Quaternary Environmental and Climatic Changes in Central Brazil.
716 *Quaternary Research*. 39(1), 90-98. <https://doi.org/10.1006/qres.1993.1011>

717 Ledru, M.-P., Braga, P.I.S., Soubiès, F., Fournier, M., Martin, L., Suguio, K., Turcq, B. 1996. The last
718 50,000 years in the Neotropics (Southern Brazil): evolution of vegetation and climate. *Palaeogeography,*
719 *Palaeoclimatology, Palaeoecology*. 123, 239-257. [https://doi.org/10.1016/0031-0182\(96\)00105-8](https://doi.org/10.1016/0031-0182(96)00105-8)

720 Ledru, M.-P., Ceccantini, G., Gouveia, S.E.M., López-Sáez, J.A., Pessenda, L.C.R., Ribeiro, A.S. 2006.
721 Millennial-scale climatic and vegetation changes in a northern Cerrado (Northeast, Brazil) since the Last
722 Glacial Maximum. *Quaternary Science Reviews*. 25, 1110-1126. doi:10.1016/j.quascirev.2005.10.005

723 Marchant, R., Almieda, L., Behling, H., Berrio, J. C., Bush, M., Cleef, A., Duivenvoorden, J., Kappelle,
724 M., De Oliveira, P., Teixeira De Oliveira Filho, A., Garcia-Lozano, S., Hooghiemstra, H., Ledru, M.-P., Markgraf,
725 V., Mancini, V., Paez, M., Prieto, A., Salgado-Labouriau, M.L. 2002. Distribution and ecology of parent taxa of

- 726 pollen lodged within the Latin American Pollen Database. *Review of Palaeobotany and Palynology*. 121, 1-75.
727 [https://doi.org/10.1016/S0034-6667\(02\)00082-9](https://doi.org/10.1016/S0034-6667(02)00082-9)
- 728 Maslin, M.A., Ettwein, V.J., Wilson, K.E., Guilderson, T. P., Burns, S.J., Leng, M.J. 2011. Dynamic
729 boundary-monsoon intensity hypothesis: evidence from the deglacial Amazon River discharge
730 record. *Quaternary Science Reviews*. 30, 3823-3833. <https://doi.org/10.1016/j.quascirev.2011.10.007>
- 731 Medeiros, M.B., Fiedler, N.C. 2004. Incêndios florestais no Parque Nacional da Serra da Canastra:
732 desafios para a conservação da biodiversidade. *Ciência Florestal*. 14, 157-168.
733 <http://dx.doi.org/10.5902/198050981815>
- 734 Medina, C.L., Sanches, M.C., Tucci, M.L.S., Sousa, C.A.F., Rogério, G., Cuzzuol, F., Joly, C.A. 2009.
735 *Erythrina speciosa* (Leguminosae-Papilionoideae) under soil water saturation: morphophysiological and
736 growth responses. *Annals of Botany*. 104, 671–680. doi:10.1093/aob/mcp159.
- 737 Mendonça, R.C., Felfili, J.M., Walter, B.M.T., Silva Júnior, M.C., Rezende, A.V., Figueira, J.S., Nogueira,
738 P.E. 2008. Flora vascular do bioma Cerrado: um “checklist” com 11.430 espécies. In: Sano, S.M., Almeida,
739 S.P., Ribeiro, J.F. (Eds.) *Cerrado: Ecologia e Flora*. v.2. Embrapa Informação Tecnológica, Brasília, p. 423-1279.
- 740 Miranda, H.S., Neto, W.N., Neves, B.M.C. 2010. Caracterização das queimadas de Cerrado. In:
741 Miranda, H.S. (Ed.) *Efeitos do regime de fogo sobre a estrutura de comunidades de Cerrado: Projeto Fogo*, Ed.
742 Ibama, Brasília, Brazil, p. 23-35. ISBN 978-85-7300-305-5
- 743 Mistry, J. 1998. Fire in the cerrado (savannas) of Brazil: an ecological review. *Progress in Physical*
744 *Geography*. 22(4), 425-448. <https://doi.org/10.1177/030913339802200401>
- 745 Moreira, A.G. 2000. Effects of fire protection on savanna structure in Central Brazil. *Journal of*
746 *Biogeography*. 27, 1021-1029. <https://doi.org/10.1046/j.1365-2699.2000.00422.x>
- 747 Motta, P.E.F., Curi, N., Franzmeier, D.P. 2002. Relation of Soils and Geomorphic Surfaces in the
748 Brazilian Cerrado In: OLIVEIRA P.S., MARQUIS R.J. (Eds.). *The cerrados of Brazil: ecology and natural history of*
749 *a neotropical savanna*. Columbia University Press, New York, p. 33-50. DOI: 10.7312/oliv12042
- 750 Novello, V.F., Cruz Júnior, F.W., Vuille, M., Karmann, I., Santos, R.V., Strikis, N.M., Wang, X., Emerick,
751 S., Paula, M.S.De, Xianglei, L., Hai, C., Edwards, R.L., Barreto, E.D.E.S. 2017. A high-resolution history of the
752 South American monsoon from last glacial maximum to the Holocene. *Scientific Reports*. 7, 44267.
753 doi:10.1038/srep44267
- 754 Oliveira-Filho, A.T., Ratter, J.A. 2002. Vegetation physiognomies and woody flora of the Cerrado
755 biome. In: Oliveira, P.S., Marquis, R.J. (Eds.). *The cerrados of Brazil: ecology and natural history of a*
756 *neotropical savanna*. Columbia University Press, New York, p. 91-120. DOI: 10.7312/oliv12042
- 757 Oliveras, I., Meirelles, S.T., Hirakuri, V.L., Freitas, C.R., Miranda, H.S., Pivello, V.R. 2013. Effects of fire
758 regimes on herbaceous biomass and nutrient dynamics in the Brazilian savanna. *International Journal of*
759 *Wildland Fire*. 22, 368-380. <https://doi.org/10.1071/WF10136>
- 760 Power, M.J., Whitney, B.S., Mayle, F.E., Neves, D.M., De Boer, E.J., Maclean, K.S. 2016. Fire, climate
761 and vegetation linkages in the Bolivian Chiquitano seasonally dry tropical forest. *Philosophical Transactions*
762 *of the Royal Society B Biological Sciences*. 371, 165. <http://dx.doi.org/10.1098/rstb.2015.0165>
- 763 Prado, L.F., Wainer, I., Chiessi, C.M., Ledru, M.-P., Turcq, B. 2013. A mid-Holocene climate
764 reconstruction for eastern South America. *Climate of the Past*. 9, 2117-2133. <https://doi.org/10.5194/cp-9-2117-2013>
- 766 Project MapBiomias - Collection 2 of Brazilian Land Cover & Use Map Series, accessed on April, 2019
767 through the link: <https://mapbiomas.org/en>.
- 768 Ramos-Neto, M.B., Pivello, V.R. 2000. Lightning Fires in a Brazilian Savanna National Park: Rethinking
769 Management Strategies. *Environmental Management*. 26(6), 675-684. DOI: 10.1007/s002670010124

770 Ratter, J.A., Bridgewater S., Atkinson R., Ribeiro J. F. 1996. Analysis of the floristic composition of the
771 Brazilian cerrado vegetation II: comparison of the woody vegetation of 98 areas. *Edinburgh Journal of*
772 *Botany*. 53, 153-180. DOI: <https://doi.org/10.1017/S0960428600002821>

773 Ribeiro, J.F., Walter, B.M.T. 2008. As principais fitofisionomias do Cerrado. In: SANO S.M., ALMEIDA
774 S.P., RIBEIRO J.F. (Eds.), *Cerrado: Ecologia e Flora*, vol.1. Embrapa Informação Tecnológica, Brasília, Brazil, p.
775 151-199.

776 Rojas, M., Arias, P. A., Flores-Aqueveque, V., Seth, A., Vuille, M. 2016. The South American monsoon
777 variability over the last millennium in climate models. *Climate of the Past*. 12, 1681–1691.
778 <https://doi.org/10.5194/cp-12-1681-2016>

779 Salgado-Labouriau, M.L., Casseti, V., Ferraz-Vicentini, K.R., Martin, L., Soubiés, F., Suguio, K., Turcq, B.
780 1997. Late Quaternary vegetational and climatic changes in cerrado and palm swamp from Central Brazil.
781 *Palaeogeography, Palaeoclimatology, Palaeoecology*. 128, 215-226. [https://doi.org/10.1016/S0031-](https://doi.org/10.1016/S0031-0182(96)00018-1)
782 [0182\(96\)00018-1](https://doi.org/10.1016/S0031-0182(96)00018-1)

783 Sato, M.N., Miranda, H.S., Maia, J.M.F. 2010. O fogo e o estrato arbóreo do Cerrado: efeitos
784 imediatos e de longo prazo. In: Miranda, H.S. (Ed.) *Efeitos do regime de fogo sobre a estrutura de*
785 *comunidades de Cerrado: Projeto Fogo*, Ed. Ibama, Brasília, Brazil, p.78-92. ISBN 978-85-7300-305-5

786 Schneider, T., Bischoff, T., Haug, G.H. 2014. Migrations and dynamics of the intertropical
787 convergence zone. *Nature*. 513(7516), 45-53. doi: 10.1038/nature13636.

788 Silva, F.A.M., Assad, E.D., Steinke, E.T., Muller, A.G. 2008. O Clima do Bioma Cerrado. In:
789 Albuquerque, A.C.S., Da Silva, A.G. (Eds). *Agricultura Tropical: Quatro décadas de inovações tecnológicas,*
790 *institucionais e políticas*. Embrapa Informações Tecnológicas, Brasília, Brazil, p. 93-148. ISBN: 978-85-7383-
791 432-1

792 Silva, V.B.S., Kousky, V.E. 2012. The South American Monsoon System: Climatology and Variability.
793 In: Wang, S-Y., Gillies, R.R. (Eds). *Modern climatology*. InTech, London, United Kingdom, p. 123-152. DOI:
794 10.5772/38565.

795 Simon, M.F., Grether, R., De Queiroz, L.P., Skema, C., Pennington, R.T, Hughes, C.E. 2009. Recent
796 assembly of the Cerrado, a neotropical plant diversity hotspot, by in situ evolution of adaptations to fire.
797 *Proceedings of the National Academy of Sciences*. 106(48), 20359–20364.
798 <https://doi.org/10.1073/pnas.0903410106>

799 Stockmarr, J. 1971. Tablets with spores used in absolute pollen analysis. *Pollen Spores*. 13, 615-621.

800 Stríkis, N.M., Chiessi, C.M., Cruz, F.W., Vuille, M., Cheng, H., Barreto, E.A.S., Mollenhauer, G., Kasten,
801 S., Karmann, I., Edwards, R.L., Bernal, J.P., Sales, H.D.R. 2015. Timing and structure of Mega-SACZ events
802 during Heinrich Stadial 1. *Geophysical Research Letters*. 42, 1-8. <https://doi.org/10.1002/2015GL064048>

803 Stríkis, N.M., Cruz, F.W., Cheng, H., Karmann, I., Edwards, R.L., Vuille, M., Wang, X., De Paula, M.S.
804 Novello, V.F. 2011. Abrupt Variations in South American Monsoon Rainfall during the Holocene based on a
805 Speleothem Record from Central-Eastern Brazil. *Geology*. 39(11), 1075-1078.

806 Stríkis, N.M., Cruz Júnior, F.W., Barrteto, E.A.S., Naughton, F., Vuille, M., Cheng, H., Voelker, A.H.L.,
807 Zhang, H., Karmann, I., Edwards, R.L., Auler, A.S., Santos, R.V., Sales, H.R. 2018. South American monsoon
808 response to iceberg discharge in the North Atlantic. *Proceedings of the National Academy of Sciences*. 115,
809 3788-3793. doi:10.1073/pnas.1717784115

810 Terra, M.C.N.S., Dos Santos, R.M., Prado Júnior, J.P., De Mello, J.M., Scolforo, J.R.C., Fontes, M.A.L.F.,
811 Schiavini, I., Dos Reis, A.A., Bueno, I.T., Magnago, L.F.S., Ter Steege, H. 2018. Water availability drives
812 gradients of tree diversity, structure and functional traits in the Atlantic–Cerrado–Caatinga transition, Brazil.
813 *Journal of Plant Ecology*. 11(6), 803-814. doi: 10.1093/jpe/rty017

814 Vera, C., Higgins, W., Amador, J., Ambrizzi, T., Garreaud, R., Gochis, D., Gutzler, D., Lettenmaier, D.,
815 Marengo, J., Mechoso, C.R., Nogues-Paegle, J., Silva Dias, P.L., Zhang, C. 2006. Toward a unified view of the
816 American Monsoon Systems. *Journal of Climate*. 19, 4977-5000. doi:10.1175/JCLI3896.1

817 Walker, M., Head, M.J., Berkelhammer, M., Björck, S., Cheng, H., Cwynar, L., Fisher, D., Gkinis, V.,
818 Long, A., Lowe, J., Newnham, R., Rasmussen, S.O., Weiss, H. 2018. Formal ratification of the subdivision of
819 the Holocene Series/Epoch (Quaternary System/Period), two new Global Boundary Stratotype Sections and
820 Points (GSSPs) and three new stages/subseries. *Episodes*. 41, 213-223.
821 <https://doi.org/10.18814/epiugs/2018/018016>

822 Wang, X., Edwards, R. L., Auler, A. S., Cheng, H., Ito, E. 2007. Millennial-scale interhemispheric
823 asymmetry of low-latitude precipitation: speleothem evidence and possible high-latitude forcing. In:
824 Schmittner, A., Chiang, J.C., Hemming, S.R. (Eds). *Ocean Circulation: Mechanisms and Impacts - Past and*
825 *Future Changes of Meridional Overturning, Geophysical Monograph Series, American Geophysical Union,*
826 *Washington, D.C., 173, 279-294. doi:10.1029/173GM18*

827 Wang, X., Edwards, R., Auler, A., Cheng, H., Kong, X., Wang, Y., Cruz, F.W., Dorale, J.A., Chiang, H.W.
828 2017. Hydroclimate changes across the Amazon lowlands over the past 45,000 years. *Nature*. 541, 204-207.
829 <https://doi.org/10.1038/nature20787>

830 Ward, B.M., Wong, C.I., Novello, V.F., Mcgee, D., Santos, R.V., Silva, L.C.R., Cruz, F.W., Wang, X.,
831 Edwards, R.L., Cheng, H. 2019. Reconstruction of Holocene coupling between the South American Monsoon
832 System and local moisture variability from speleothem $\delta^{18}\text{O}$ and $^{87}\text{Sr}/^{86}\text{Sr}$ records. *Quaternary Science*
833 *Reviews*. 210, 51-63. <https://doi.org/10.1016/j.quascirev.2019.02.019>

834 Willard, D., Bernhardt, C.E., Weimer, L.G., Cooper, S.R., Gámez, D., Jensen, J.A. 2004. Atlas of pollen
835 and spores of the Florida Everglades. *Palynology*. 28, 175–227. doi/abs/10.1080/01916122.2004.9989597

836

837

838 **List of tables**

839 **Table 01:** Radiocarbon dates of the LF15-2 core.

840

841 **List of figures**

842 **Figure 01:** Geographic distribution and climate of the Cerrados, locations from which pollen and isotopic records
843 mentioned in this study were collected, and geology and vegetation of the Lagoa Feia site..

844 **Figure 02:** Lithology and age-depth model for the LF15-2 sediment core.

845 **Figure 03:** XRF scanning results showing the levels of selected elements (Zr, Si, Rb, K, Al, Fe, Zn, Ti, Ca, Sr, S), along
846 with relevant ratios (Rb/K, Fe/Ti, Zn/Ti, Si/Ti, Ca/Ti, S/Ti), for core LF15-2 plotted against depth.

847 **Figure 04:** Synthetic pollen percentage diagram for the LF15-2 core, with data plotted against depth (y-axis).

848 **Figure 05:** Summary pollen diagram for the LF15-2 core, with the data plotted against time (cal yr BP).

849 **Figure 06:** Synthetic representation of paleoecological changes over the last 16,000 years observed from the
850 Lagoa Feia (this study), São José and Salitre cores (from Cassino et al., 2018 and Ledru, 1993, respectively).

851 **Figure 07:** Principal Components Analysis of interpolated pollen data from Lagoa Feia, São José and Salitre
852 records.

853 **Figure 08:** Comparison of vegetation cover variability in central Cerrados and δO_{18} speleothem records from
854 adjacent regions.

855 **Figure 09:** Schematic representation of SASM position and activity during the Pleistocene-Holocene transition and
856 early-middle Holocene in central Cerrados.

857

858

860 **Supplementary Material**

861 Table 1: List of pollen taxa identified from the Lagoa Feia core

Pollen taxa	Family	Habitat (Cerrados physiognomy) ¹	Life-form type ^{1,2}
<i>Acacia</i> -Type	Fabaceae	forest, savanna, dry forest	tree, bindweed
<i>Acalypha cf. diversifolia</i>	Euphorbiaceae	forest	shrub
<i>Acalypha</i> sp.	Euphorbiaceae	grassland, forest	shrub, herb
<i>Acosmium</i> -Type	Fabaceae	savanna, dry forest, forest, grassland	tree, shrub
<i>Alchornea</i> sp.	Euphorbiaceae	forest	tree
<i>Alternanthera</i> sp.	Amaranthaceae	grassland, savanna, forest, swamp	herb, subshrub
<i>Amaranthus</i> -Type	Amaranthaceae	-	herb
<i>Anadenanthera</i> -Type	Fabaceae	forest, dry forest	tree
<i>Andira</i> -Type	Fabaceae	forest, dry forest, savanna	tree, shrub
Annonaceae	Annonaceae	savanna, dry forest, forest, grassland, swamp	tree, shrub, subshrub
<i>Aphelandra</i> sp.	Acanthaceae	-	shrub, herb, subshrub
<i>Apuleia leiocarpa</i>	Fabaceae	forest	tree
Asteraceae	Asteraceae	grassland, savanna, dry forest, forest, swamp, palm swamp	all
<i>Astronium</i> -Type	Anacardiaceae	savanna, forest	tree
<i>Attalea</i> -Type	Arecaceae	savanna, forest	shrub, tree
<i>Banisteriopsis</i> -Type	Malpighiaceae	savanna, forest, grassland	shrub, bindweed, subshrub, tree
<i>Bauhinia</i> sp.	Fabaceae	forest, savanna, grassland, dry forest	shrub, subshrub, bindweed
<i>Begonia</i> sp.	Begoniaceae	forest, grassland	herb
<i>Borreria</i> -Type	Rubiaceae	savanna, grassland	herb, subshrub, shrub
<i>Brosimum</i> -Type	Moraceae	savanna, grassland, forest	shrub, tree
<i>Byrsonima</i> sp.	Malpighiaceae	savanna, forest, grassland, swamp, palm swamp, dry forest	tree, shrub, subshrub, herb,
Cactaceae	Cactaceae	savanna, forest	herb, shrub
<i>Callisthene</i> sp.	Vochysiaceae	forest, savanna, dry forest	tree
<i>Calophyllum</i> sp.	Clusiaceae	forest	tree
<i>Caperonia</i> sp.	Euphorbiaceae	aquatic	herb
<i>Caryocar brasiliense</i>	Caryocaraceae	savanna, dry forest	tree
<i>Casearia</i> sp.	Flacourtiaceae	grassland, savanna, forest, dry forest	tree, shrub
<i>Cecropia</i> sp.	Cecropiaceae	forest, savanna	tree

<i>Cedrela</i> -Type	Meliaceae	forest	tree
<i>Celtis</i> sp.	Ulmaceae	forest	tree
<i>Centrosema</i> sp.	Fabaceae	savanna, grassland, forest	bindweed, subshrub
<i>Cestrum</i> sp.	Solanaceae	forest, savanna, dry forest, grassland	shrub, subshrub
<i>Chrysophyllum</i> sp.	Sapotaceae	savanna, forest	tree
<i>Cissampelos</i> sp.	Menispermaceae	forest, grassland, savanna	bindweed, herb, subshrub
<i>Cissus</i> sp.	Vitaceae	forest, savanna	bindweed
<i>Commiphora leptophloeos</i>	Burseraceae	forest	tree
<i>Copaifera</i> sp.	Fabaceae	savanna, forest, dry forest	tree, shrub
<i>Cordia</i> sp.	Boraginaceae	savanna, grassland, forest, dry forest	tree, shrub, subshrub
<i>Crotalaria</i> -Type	Fabaceae	forest, savanna, grassland, swamp	shrub, subshrub, herb
<i>Croton</i> -Type	Euphorbiaceae	savanna, dry forest, grassland, forest	herb, tree, subshrub, shrub
<i>Cuphea</i> sp1.	Lythraceae	grassland, savanna, palm swamp, forest, dry forest, swamp	herb, subshrub
<i>Cuphea</i> sp2.	Lythraceae	grassland, savanna, palm swamp, forest, dry forest, swamp	herb, subshrub
<i>Curatella americana</i>	Dilleniaceae	savanna, dry forest	tree
Cyperaceae	Cyperaceae	forest, grassland, swamp, palm swamp, savanna, dry forest	herb
<i>Dendropanax</i> sp.	Araliaceae	forest	tree
<i>Desmodium</i> sp.	Fabaceae	savanna, grassland, dry forest, forest	subshrub, herb, shrub
<i>Dilodendron bipinnatum</i>	Sapindaceae	forest	tree
<i>Diodia</i> -Type	Rubiaceae	savanna, grassland, forest	subshrub, shrub, herb
<i>Doliocarpus</i> -Type	Dilleniaceae	forest, dry forest	bindweed
<i>Drimys</i> sp.	Winteraceae	forest, grassland	tree
<i>Drosera</i> sp.	Droseraceae	swamp, grassland	herb
<i>Drymaria</i> sp.	Caryophyllaceae	swamp	herb
<i>Echinodorus</i> sp.	Alismataceae	swamp, (palm swamp, savanna, forest)	herb
<i>Eichornia</i> sp.	Pontederidaceae	aquatic	herb
Ericaceae	Ericaceae	forest, savanna, swamp, grassland	shrub, tree, subshrub
Eriocaulaceae	Eriocaulaceae	swamp, grassland, savanna, forest, palm swamp	herb, subshrub
<i>Eriotheca</i> -Type	Malvaceae	forest, savanna	tree
<i>Eryngium</i> -Type	Apiaceae	forest, swamp, savanna, grassland	herb
<i>Erythrina</i> cf. <i>speciosa</i>	Fabaceae	savanna, forest	tree

<i>Erythroxylum</i> sp.1	Erythroxylaceae	forest, savanna, grassland, dry forest, swamp	tree, herb, shrub, subshrub
<i>Erythroxylum</i> sp.2	Erythroxylaceae	forest, savanna, grassland, dry forest, swamp	tree, herb, shrub, subshrub
<i>Euphorbia</i> sp.	Euphorbiaceae	savanna, swamp, grassland	herb, tree
<i>Euplassa</i> sp.	Proteaceae	forest, savanna	tree
<i>Evolvulus</i> sp.	Convolvulaceae	forest, savanna, grassland, dry forest, swamp	herb, subshrub
<i>Ficus</i> sp.	Moraceae	forest	tree
<i>Forsteronia</i> -Type	Apocynaceae	forest, dry forest	tree, bindweed
<i>Friedericia</i> sp.	Bignoniaceae	forest	bindweed
<i>Galianthe</i> sp.	Rubiaceae	grassland, swamp	herb, subshrub
<i>Gomphrena</i> sp.	Amaranthaceae	savanna, grassland, forest, swamp	subshrub, herb
<i>Gomphrena</i> sp.2	Amaranthaceae	savanna, grassland, forest, swamp	subshrub, herb
<i>Gouania</i> -Type	Rhamnaceae	savanna, forest	bindweed
<i>Hedyosmum brasiliense</i>	Chloranthaceae	forest, swamp	tree
<i>Helicteres</i> sp.	Malvaceae	forest, savanna, grassland	shrub, subshrub
<i>Hyeronima</i> sp.	Euphorbiaceae	forest	tree
<i>Hyptis</i> -Type	Lamiaceae	grassland, savanna, swamp, dry forest, forest, palm swamp	herb, shrub, subshrub
<i>Ilex</i> sp.	Aquifoliaceae	forest, savanna, grassland	tree, shrub
Iridaceae	Iridaceae	grassland, swamp, dry forest	herb
<i>Jacaranda</i> -Type	Bignoniaceae	savanna, forest, grassland, dry forest	tree, shrub, subshrub
<i>Jacquemontia</i> -Type	Convolvulaceae	savanna, forest	herb, bindweed
<i>Lamanomia</i> sp.	Cunoniaceae	forest	tree, shrub
<i>Laplacea</i> sp.	Theaceae	forest, grassland	tree
<i>Lippia</i> sp.	Verbenaceae	grassland, savanna, forest, swamp	shrub, herb, subshrub
<i>Lobelia</i> -Type	Campanulaceae	grassland, savanna, swamp, forest	herb, subshrub
<i>Ludwigia</i> sp.	Onagraceae	grassland, swamp, forest	herb, subshrub, shrub
<i>Machaerium</i> -Type	Fabaceae	forest, savanna, dry forest	tree
<i>Maprounea</i> -Type	Euphorbiaceae	forest, savanna, dry forest	shrub
<i>Matayba</i> sp.	Sapindaceae	forest, savanna, dry forest	tree, shrub, bindweed
<i>Mauritia flexuosa</i>	Arecaceae	palm swamp, swamp	tree
<i>Maytenus</i> -Type	Celastraceae	forest, savanna	tree, shrub
Melastomataceae	Melastomataceae	All	all

<i>Melochia</i> sp.	Malvaceae	savanna, forest, grassland	subshrub, herb, shrub
<i>Mimosa</i> sp.1	Fabaceae	savanna, grassland, forest, palm swamp, dry forest,	shrub, tree, herb, subshrub
<i>Mimosa</i> sp.2	Fabaceae	savanna, grassland, forest, palm swamp, dry forest,	shrub, tree, herb, subshrub
<i>Myriophyllum</i> sp.	Haloragaceae	swamp, aquatic	herb
<i>Myrocarpus</i> sp.	Fabaceae	forest	tree
<i>Myroxylon</i> sp.	Fabaceae	forest	tree
<i>Myrsine</i> sp.	Myrsinaceae	forest, dry forest, savanna	tree
Myrtaceae	Myrtaceae	forest, savanna, dry forest, grassland, palm swamp	tree, subshrub, shrub
Nymphaeaceae	Nymphaeaceae	aquatic	herb
<i>Parinari</i> sp.	Chrysobalanaceae	savanna, grassland	shrub
<i>Peperomia</i> sp.	Piperaceae	forest	herb
<i>Peritassa</i> -Type	Celastraceae	forest, savanna	shrub, bindweed
<i>Pfaffia</i> sp.	Amaranthaceae	savanna, grassland	herb, shrub
<i>Phyllanthus</i> sp.1	Phyllanthaceae	savanna, dry forest, grassland, forest	shrub, herb, subshrub
<i>Phyllanthus</i> sp.2	Phyllanthaceae	savanna, dry forest, grassland, forest	shrub, herb, subshrub
<i>Piper</i> sp.	Piperaceae	forest	shrub, tree, herb
<i>Piptadenia</i> sp.	Fabaceae	forest, savanna	tree
<i>Plenckia populnea</i>	Celastraceae	savanna, forest	tree
Poaceae	Poaceae	all	herb
<i>Podocarpus</i> sp.	Podocarpaceae	forest	tree
<i>Poeppigia procera</i>	Fabaceae	savanna	shrub
<i>Polygala</i> sp.	Polygalaceae	grassland, savanna, forest, swamp, palm swamp	herb, subshrub, shrub
<i>Polygonum</i> cf. <i>meisnerianum</i>	Polygonaceae	savanna, aquatic	herb
<i>Pontederia</i> sp.	Pontederidaceae	aquatic, swamp	herb
<i>Pouteria</i> sp.	Sapotaceae	savanna, forest, palm swamp	tree, shrub
<i>Protium</i> sp.	Burseraceae	savanna, forest, dry forest	tree, shrub
<i>Prunus</i> sp.	Rosaceae	forest	tree
<i>Pseudobombax</i> cf. <i>longiflorum</i>	Malvaceae	dry forest	tree
<i>Pseudobombax</i> cf. <i>marginatum</i>	Malvaceae	savanna	tree
<i>Pterogyne nitens</i>	Fabaceae	savanna	tree
<i>Pyrostegia</i> cf. <i>venusta</i>	Fabaceae	savanna, forest	bindweed

<i>Rhamnus</i> -Type	Rhamnaceae	savanna, forest	tree, shrub
<i>Roupala</i> sp.	Proteaceae	savanna, forest, dry forest	tree, shrub
<i>Sagittaria</i> sp.	Alismataceae	swamp, aquatic	herb
<i>Sapium</i> sp.	Euphorbiaceae	savanna, forest, grassland	tree, shrub, subshrub
<i>Sauvagesia</i> sp.	Ochnaceae	savanna, swamp	shrub, subshrub
<i>Schefflera</i> sp.	Araliaceae	forest, savanna	tree
<i>Schinus</i> sp.	Anacardiaceae	savanna, dry forest, forest	tree, shrub
<i>Sclerolobium</i> -Type	Fabaceae	savanna, forest	tree
<i>Sebastiania</i> sp.	Euphorbiaceae	savanna, forest, grassland	herb, subshrub, shrub, tree
<i>Senna</i> -Type	Fabaceae	savanna, forest	shrub, subshrub, tree, herb
<i>Serjania</i> sp.	Sapindaceae	forest, savanna, dry forest	bindweed
<i>Sida</i> -Type	Malvaceae	savanna	shrub, herb
<i>Sloanea</i> sp.	Elaeocarpaceae	forest	tree
<i>Solanum</i> sp.	Solanaceae	savanna, forest	all
<i>Sterculia</i> sp.	Malvaceae	forest	tree
<i>Stryphnodendron</i> sp.	Fabaceae	savanna, grassland	tree, shrub
<i>Styrax</i> sp.	Styracaceae	forest, savanna	tree, shrub
<i>Syagrus</i> -Type	Arecaceae	savanna, grassland, dry forest, forest	tree, shrub
<i>Symplocos</i> sp.1	Symplocaceae	forest, dry forest, savanna	tree
<i>Symplocos</i> sp.2	Symplocaceae	forest, dry forest, savanna	tree
<i>Tabebuia</i> -Type	Bignoniaceae	savanna, forest	tree, shrub
<i>Tapirira</i> sp.	Anacardiaceae	forest, savanna	tree
<i>Toulicia</i> -Type	Sapindaceae	savanna	shrub, subshrub
<i>Trema micrantha</i>	Ulmaceae	forest	tree
<i>Typha</i> sp.	Typhaceae	swamp, aquatic	herb
<i>Urera</i> -Type	Moraceae	forest	shrub
<i>Utricularia</i> sp.	Lentibulariaceae	grassland, swamp, aquatic	herb
<i>Vismia</i> sp.	Clusiaceae	forest	tree, shrub
<i>Vochysia</i> sp.	Vochysiaceae	forest, savanna, dry forest, grassland	tree, shrub
<i>Weinmannia</i> sp.	Cunoniaceae	forest	tree, shrub
<i>Xyris</i> sp.	Xyridaceae	grassland, swamp	herb

Zanthoxylum sp.	Rutaceae	forest, dry forest	tree
-----------------	----------	--------------------	------

¹ from MENDONÇA, R.C.; FELFILI, J.M.; WALTER, B.M.T.; SILVA JÚNIOR, M.C.; REZENDE, A.V.; FIGUEIRA, J.S.; NOGUEIRA, P.E. 2008. Flora vascular do bioma Cerrado: um “checklist” com 11.430 espécies. In: SANO, S.M.; ALMEIDA, S.P.; RIBEIRO, J.F. (eds.), Cerrado: Ecologia e Flora. v.2. Embrapa Informação Tecnológica, Brasília, Brazil, pp. 423-1279.

² from Flora do Brasil 2020. Jardim Botânico do Rio de Janeiro. Available at: < <http://floradobrasil.jbrj.gov.br/> >.

862

863

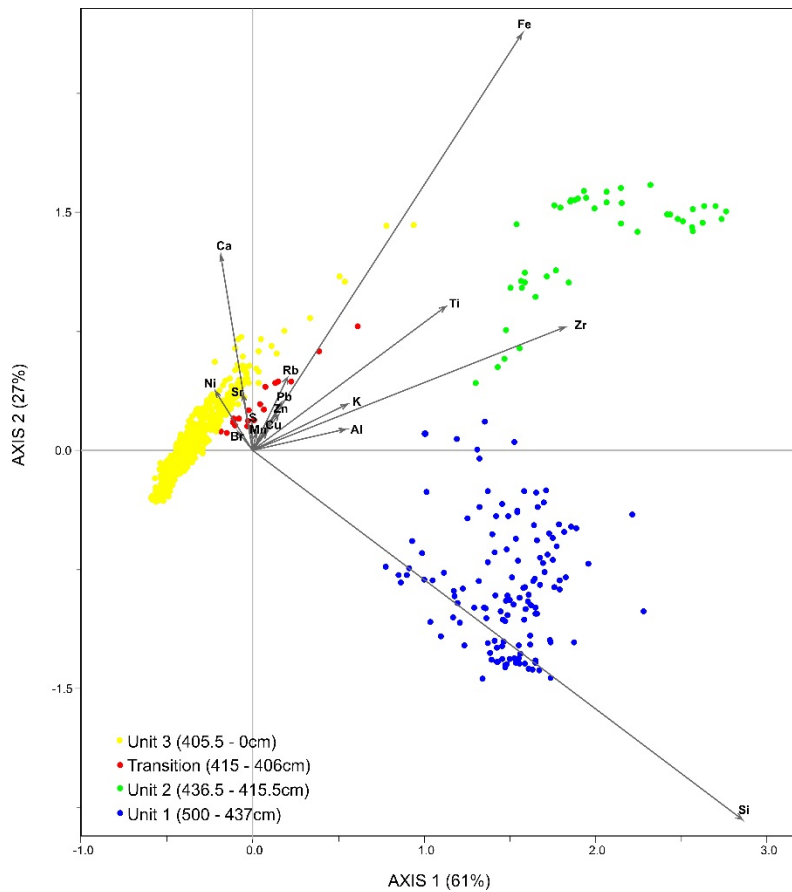
864

865

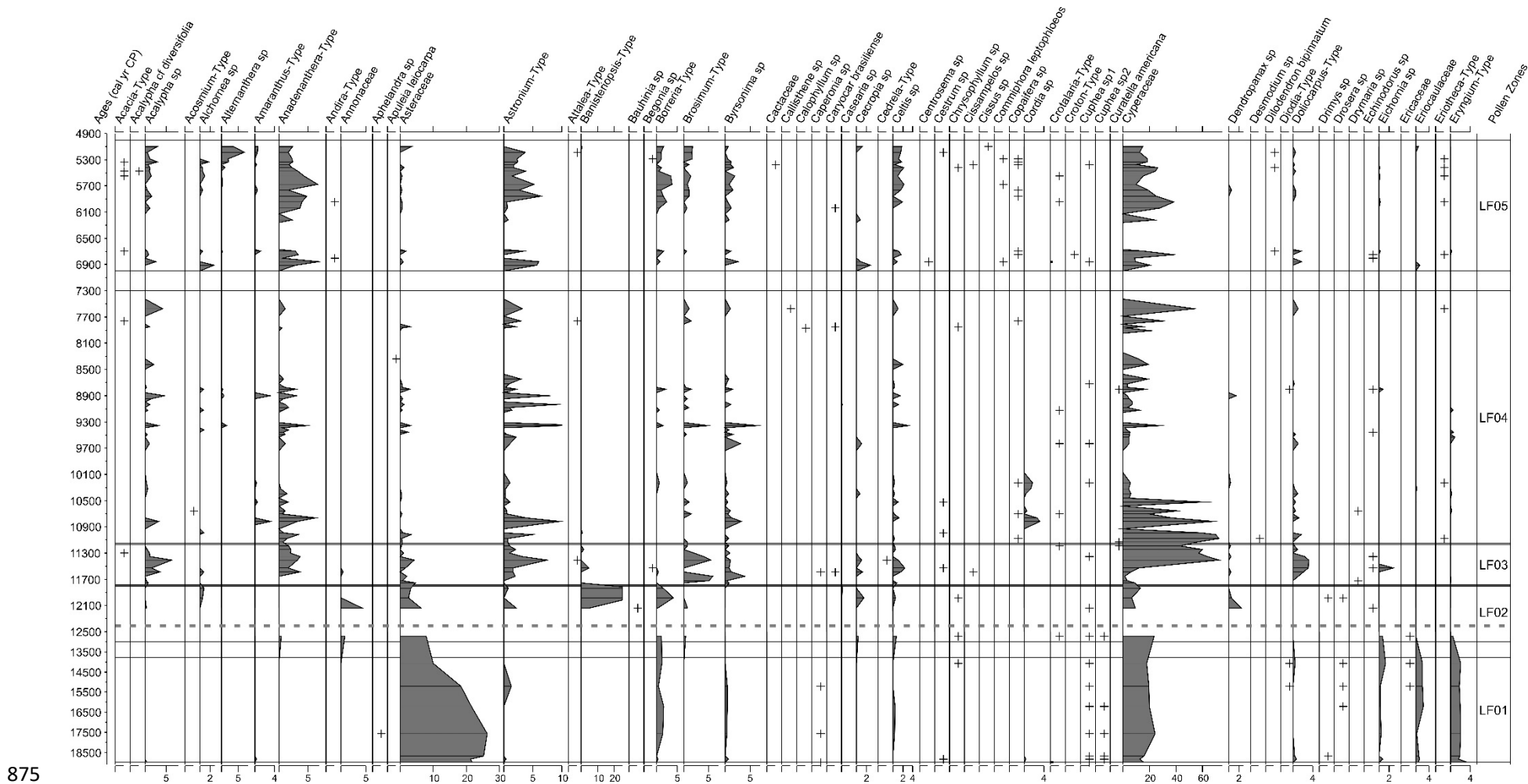
866

867

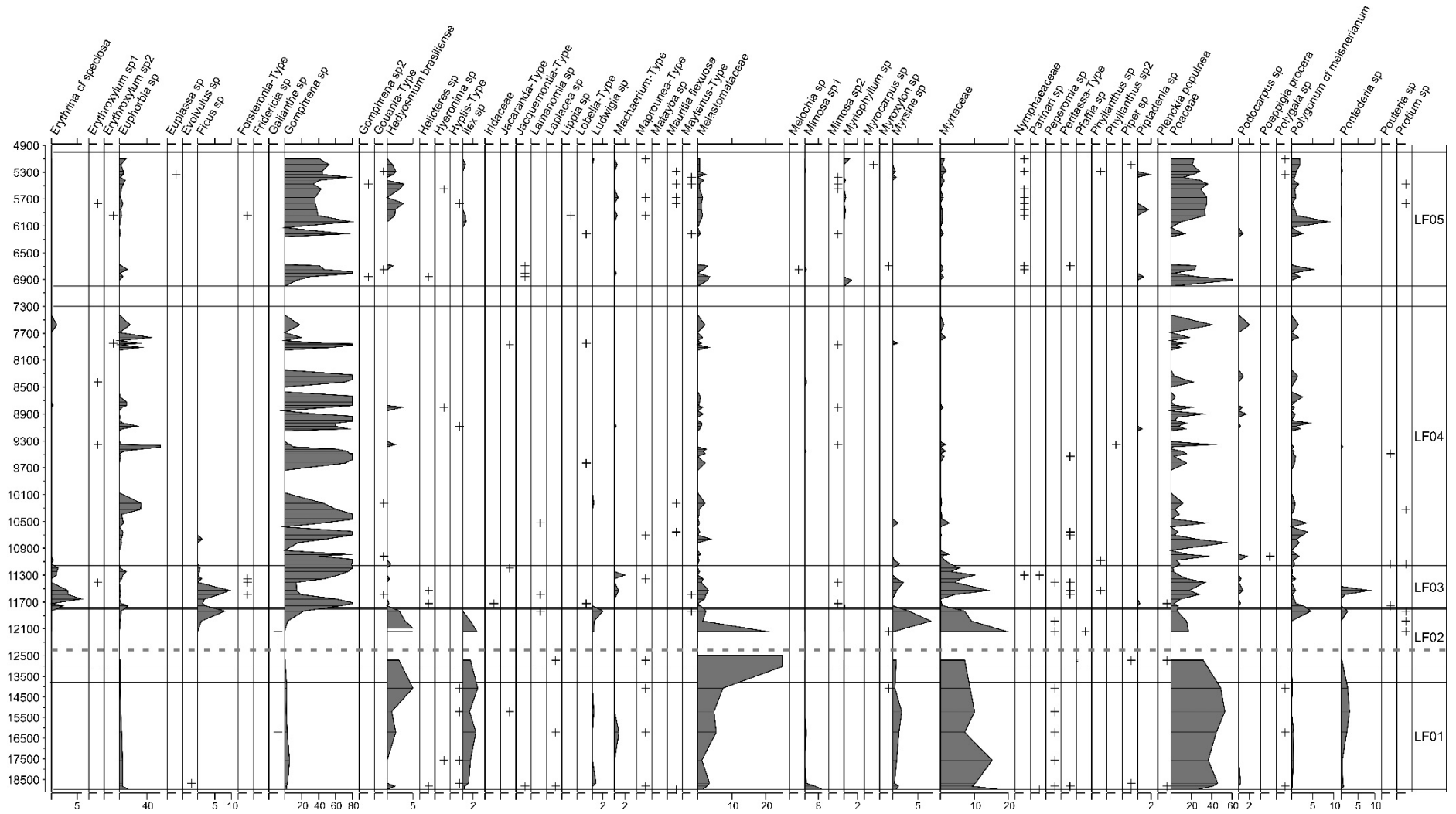
868



869
 870 **Figure 1:** Principal Components Analysis biplot of the most significant elements detected through XRF scanning of the
 871 LF15-2 core. Samples from units 1, 2, and 3 are plotted in blue, green, and yellow, respectively, with the red color
 872 denoting samples at the transition phase from unit 2 to 3.
 873

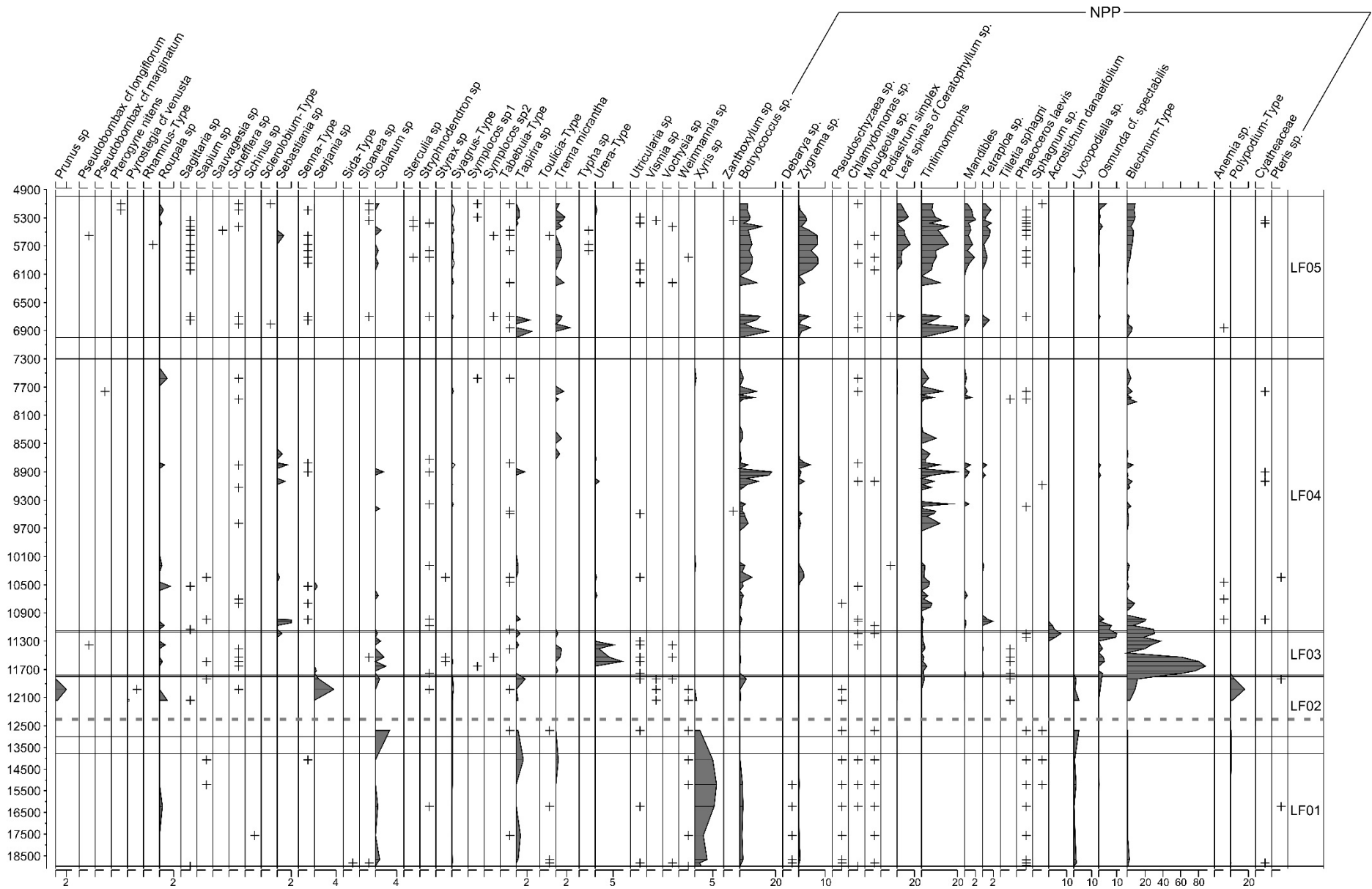


876 **Figure 2:** Complete percentage diagram for the Lagoa Feia record with all pollen and non-pollen palynomorphs (NPP). Pollen taxa are presented in alphabetic order. The
 877 bottom part of the core (section below the dashed horizontal line) has a compressed age scale.



879

880 **Figure 3:** Complete percentage diagram for the Lagoa Feia record with all pollen and non-pollen palynomorphs (NPP). (cont.)

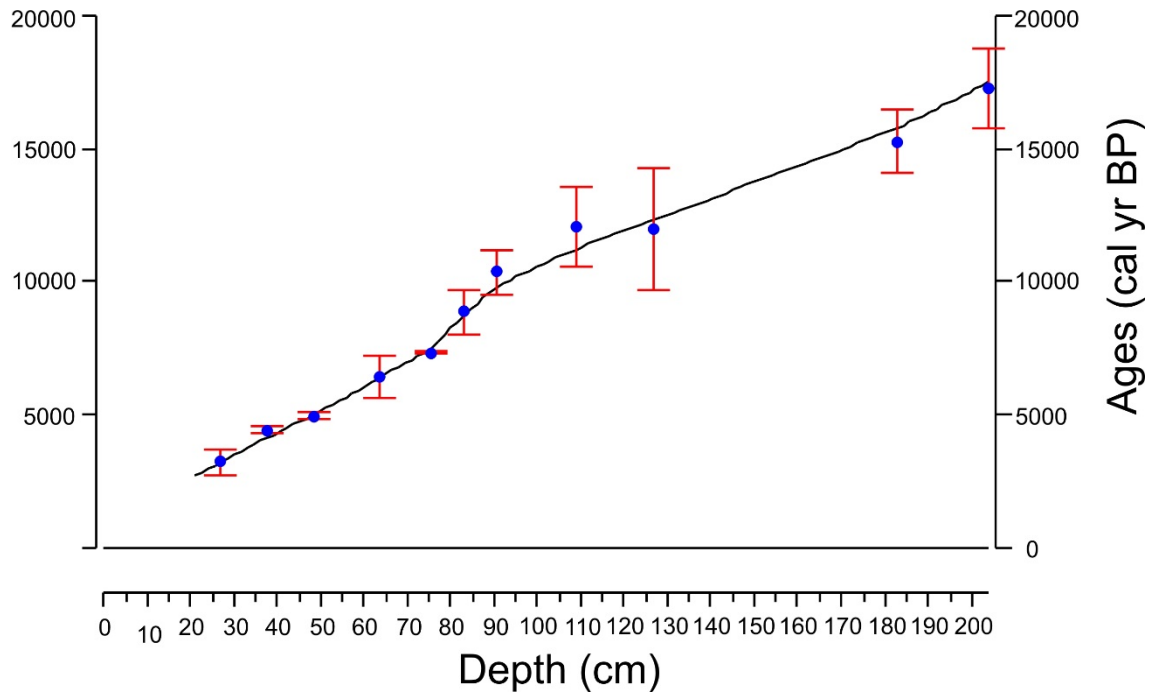


881

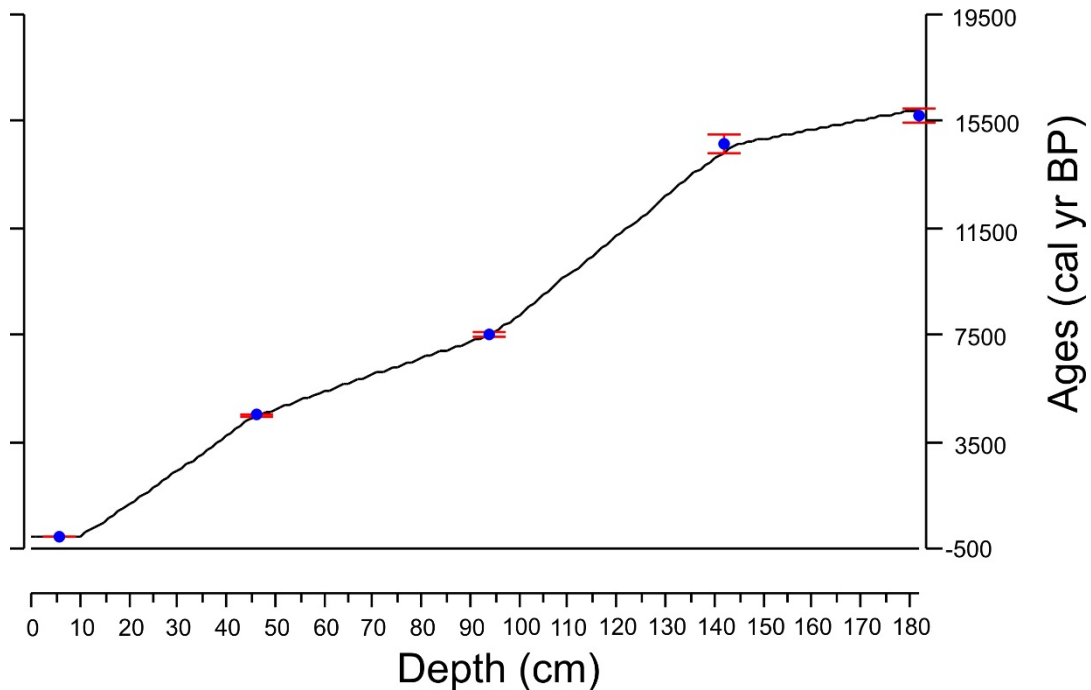
882 **Figure 4:** Complete percentage diagram for the Lagoa Feia record with all pollen and non-pollen palynomorphs (NPP). (cont.)

97

98



883
 884 **Figure 5:** Age-depth model for the Salitre record (Ledru, 1993; Ledru *et al.*, 1996). The Salitre record consists of a 6m
 885 core collected from a peat bog located on the top of a circular elevated area (1100 m) associated to a carbonatite plug,
 886 situated in western Minas Gerais State, Southeastern Brazil (19°S, 46°46'W). The core dates back to more than 50,000
 887 yr BP, but the presented age-depth model only considered the upper part of the core, spanning the period between
 888 ~2,700 and 16,000 cal yr BP. The chronology of this part of the core is based on ten radiocarbon dates and the new age-
 889 depth model was built using Bacon (Blaauw & Christen, 2011).
 890
 891



892
 893 **Figure 6:** Age-depth model for the São José record (Cassino *et al.*, 2018). The São José record consists of a 1.82 m core
 894 collected on the border zone of a *vereda* (palm swamp) located in northern Minas Gerais State (17°04'S, 45°06'W). Five
 895 radiocarbon dates were available for this core and were used to build the age-depth model with Bacon (Blaauw &
 896 Christen, 2011).